JOURNAL OF Materials Feature Article CHEMISTRY

Donor–acceptor complexes of fullerene C_{60} with organic and organometallic donors†

Dmitri V. Konarev,[a] Rimma N. Lyubovskaya,*[a] Natal'ya V. Drichko,[b] Evgeniya I. Yudanova,[a] Yury M. Shul'ga,[a] Aleksey L. Litvinov,[a] Viktor N. Semkin[b] and Boris P. Tarasov[a]

[a]*Institute of Problems of Chemical Physics RAS, Chernogolovka, Moscow region, 142432, Russia. E-mail: lyurn@icp.ac.ru*
[b]*A. F. Ioffe Physical-Technical Institute, St.-Petersburg 194021, Russia*

Received 2nd September 1999, Accepted 23rd November 1999
Published on the Web 24th February 2000

The paper presents data on the synthesis, IR, electronic, X-ray photoelectron, and ESR spectroscopies of fullerene C_{60} molecular complexes with various types of donor compounds, namely, substituted tetrathiafulvalenes, aromatic hydrocarbons, diazodithiafulvalene, tetraphenyldipyranylidene, tetrasulfur tetranitride, saturated amines, some metallocenes, and Co(II) and Mn(II) tetraphenylporphyrins. Crystal structures of some of these complexes are discussed. The degree of charge transfer in the complexes is evaluated from the shift of the $F_{1u}(4)$ C_{60} mode in the IR spectra. The factors responsible for the appearance of the symmetry-forbidden C_{60} vibrations and the splitting of the absorption bands of C_{60} in the complexes are considered. The electronic absorption spectra of some complexes show the decrease of the intensity of electron transitions of C_{60} at 420–530 nm and the appearance of new absorption bands attributed to charge transfer from the donor to C_{60}. The dependences of the energy of charge transfer in the C_{60} complexes on ionisation and redox potentials of substituted tetrathiafulvalenes are derived. Peculiarities of donor–acceptor interaction of donor molecules with the spherical C_{60} are considered.

1 Introduction

Fullerene C_{60}[1] is known to be an acceptor and, like organic planar π-acceptors such as tetracyanoethylene (TCNE) and tetracyanoquinodimethane (TCNQ), to be capable of forming donor–acceptor complexes.[2–4] In contrast to planar acceptors, fullerenes possess a number of characteristic features, namely, spherical shape, unique electronic structure, high symmetry and polarizability.[2] These features provide a certain amount of specificity of the donor–acceptor interaction of fullerenes.

Fullerene compounds can be divided into several groups according to the degree of charge transfer (δ), though there is no distinct boundary between these groups. Solvates and clathrates of fullerene with solvents and molecular complexes of fullerene with various donors have δ close to zero.[3] In the case of partial charge transfer from the donor to fullerene ($0<\delta<1$), charge transfer complexes ($D^{+\delta}C_{60}^{-\delta}$) are formed.[2–4] Fullerene ion radical salts are characterised by complete charge transfer ($D^{+n}C_{60}^{-n}$), where n mainly is an integer.[2–8]

Donor–acceptor complexes of C_{60} demonstrate a wide range of physical properties,[2,3] including metallic[9] and probably superconducting,[10] and unusual magnetic properties (ferromagnetism with $T_c = 16.1$ K in the C_{60} salt with an organic donor TDAE (tetrakis(dimethylamino)ethylene)[11] and antiferromagnetism[12]). Intercalation of neutral C_{60} complexes by alkali metals can result in the formation of superconductors which in contrast to the three-dimensional superconductors M_3C_{60} (K, Rb, Cs) have one- or two-dimensional structures.[13,14]

Conducting polymer composites with C_{60} provided the design of novel materials, in which an effective charge transfer from the excited polymer to C_{60} and charge separation states with long lifetimes are possible. This phenomenon can be used in xerography and solar energy phototransducers.[15] The studies of charge phototransfer in the C_{60} complexes in the solid state also show the possibility of charge separation states with long lifetimes.[16] Now the luminescent[17] and nonlinear optical properties[18] of fullerene complexes and composites with organic donors are being studied.

There are now publications on the syntheses, crystal structures and some properties of the C_{60} complexes with inorganic compounds, namely, phosphorus, $(P_4)_2C_{60}$;[19] sulfur, $(S_8)_2C_{60}$;[20] and iodine, $I_2{\cdot}C_{60}{\cdot}C_6H_5CH_3$;[21] organic donors, namely, bis(ethylenedithio)tetrathiafulvalene, $(BEDT\text{-}TTF)_2C_{60}$;[22] octamethylenetetrathiafulvalene, $OMTTF{\cdot}C_{60}{\cdot}C_6H_6$;[23] tetramethyltetraselenafulvalene, $TMTSeF{\cdot}C_{60}(C_6H_6)_{0.5}$ and $TMTSeF{\cdot}C_{60}(CS_2)_2$;[24,25] bis(ethylenethio)-tetrathiafulvalene, $BET\text{-}TTF{\cdot}C_{60}{\cdot}C_7H_8$;[26] bis(dimethylthieno) tetratellurafulvalene, $BDMT\text{-}TTeF{\cdot}C_{60}{\cdot}CS_2$;[27] bis(methylthio) ethylenedithiotetrathiafulvalene, $(C_1TET\text{-}TTF)_2C_{60}$;[28] twin-bis(ethylenedithio)tetrathiafulvalene, $twin\text{-}BEDT\text{-}TTF{\cdot}C_{60}{\cdot}CS_2$;[29] hexamethoxycyclotriveratrylene, $CTV{\cdot}C_{60}$[30] and $CTV(C_{60})_{1.5}(C_7H_8)$;[31] hexamethoxytriphenylene, $(HMT)_2C_{60}$;[32] substituted calix[3]arenes,[33] calix[4]arenes[34] and calix[5] arenes;[35] calix[4]resorcinarene;[36] *N*,*N*,*N*′,*N*′-tetramethyl-*p*-phenylenediamine, $TMPD{\cdot}C_{60}$;[37,38] tetrakis(dimethylamino) ethylene, $TDAE{\cdot}C_{60}$;[4,39] octakis(dimethylamino)porphirazine, $(ODMAPz)_2C_{60}$;[40] 3,3′,4,4′-tetrathiabis(1,2,5-thiadiazole), $(twin\text{-}TDAS)_4(C_{60})_3$;[41] hydroquinone, $(HQ)_3C_{60}$;[42] octaphenylcyclotetrasiloxane, $[\{SiPh_2(\mu\text{-}O)\}_4]C_{60}(C_7H_8)_{0.5}$;[43] organometallic donors, namely, triphenylantimony, $(Ph_3Sb)_6C_{60}$;[44] ferrocene, $(Cp_2Fe)_2C_{60}$;[45] decamethylnickelocene, $Cp^*_2Ni{\cdot}C_{60}{\cdot}CS_2$;[46] cobaltocene, $Cp_2Co{\cdot}C_{60}{\cdot}CS_2$;[47] $(Cp)_4Fe(CO)_4{\cdot}C_{60}(C_6H_6)_3$;[48] (tetraphenylporphinato)chromium(III), $CrTPP{\cdot}C_{60}(THF)_3$,[49] and some nickel(II) macrocycles.[50]

This paper summarises our own results on the studies of C_{60} complexes with organic and organometallic donors. We used substituted tetrathiafulvalenes, aromatic hydrocarbons, diazodithiafulvalenes, tetraphenyldipyranylidenes, tetrasulfur tetranitride, saturated amines, and a number of metallocenes and metal(II) tetraphenylporphyrins as donors. The synthesis of a great number of C_{60} complexes enabled us to find some features of donor–C_{60} interactions and charge transfer in these compounds, to understand the reasons of C_{60} symmetry

†Characteristics of C_{60} complexes are available as supplementary data. For direct electronic access see http://www.rsc.org/suppdata/jm/a9/a907106g

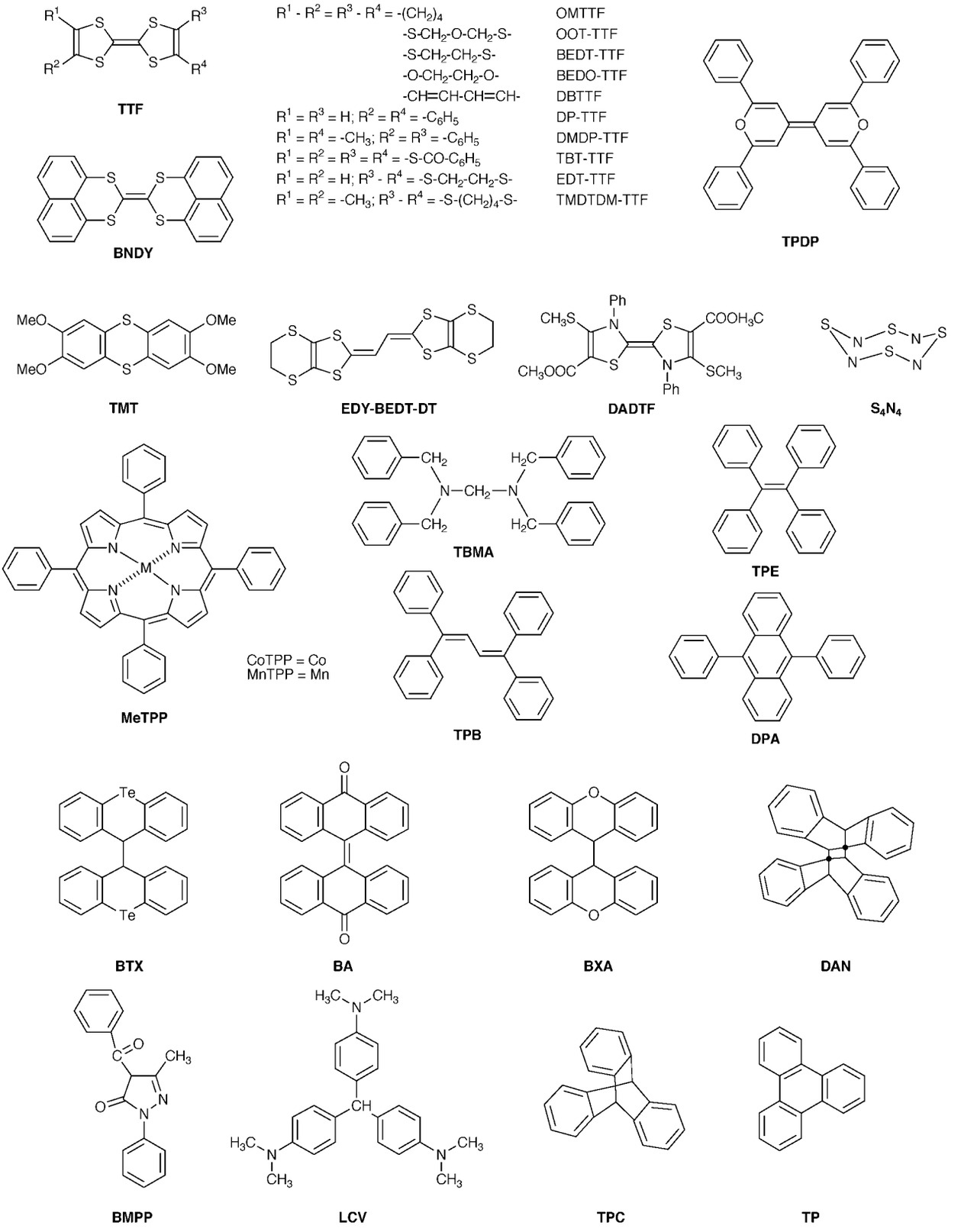

Fig. 1 Donor compounds and their abbreviations: OMTTF: octamethylenetetrathiafulvalene; OOT-TTF: bis(oxydimethylenedithio)tetrathiafulvalene; BEDT-TTF: bis(ethylenedithio)tetrathiafulvalene; BEDO-TTF: bis(ethylenedioxo)tetrathiafulvalene; DBTTF: dibenzotetrathiafulvalene; DP-TTF: 4,4′-diphenyltetrathiafulvalene; DMDP-TTF: *trans*-4,4′-dimethyl-5,5′-diphenyltetrathiafulvalene; TBT-TTF: 4,4′,5,5′-tetrakis(benzoylthio)tetrathiafulvalene; EDT-TTF: ethylenedithiotetrathiafulvalene; TMDTDM-TTF: tetramethylenedithio-4,5-dimethyltetrathiafulvalene; BNDY: binaphtho[1,6-*de*]-1,3-dithiin-2-ylidene; TPDP: 3,3′,5,5′-tetraphenyldipyranylidene; EDY-BEDT-DT: 2,2′-ethanediylidenebis(4,5-ethylenedithio-1,3-dithiole); DADTF: 2,2′-bi(4-methylthio-3-phenyl-5-methoxycarbonyl-1,3-thiazolinylidene); TMT: 2,3,7,8-tetramethoxythianthrene; CoTPP: 5,10,15,20-tetraphenyl-21*H*,23*H*-porphinecobalt(II); MnTPP: 5,10,15,20-tetraphenyl-21*H*,23*H*-porphinemanganese(II); S_4N_4: tetrasulfur tetranitride; TBMA: *N*,*N*′,*N*,*N*′-tetrabenzylmethanediamine; TPE: tetraphenylethylene; TPB: tetraphenylbutadiene; DPA: 9,10-diphenylanthracene; BTX: *trans*-9,9′-bis(telluraxanthenyl); BA: bianthrone; BXA: bixanthene; DAN: dianthracene; (5,6,11,12-tetrahydro-5,12-[1′,2′]:6,11-[1″,2″]-dibenzenodibenzo[*a*,*e*]cyclooctene); BMPP: 4-benzoyl-3-methyl-1-phenyl-2-pyrazoline-5-one; LCV: 4,4′,4″-methylidynetris(*N*,*N*′-dimethylaniline); TPC: triptycene (9,10-*o*-benzeno-9,10-dihydroanthracene); TP: triphenylene; DBA: 1,2:5,6-dibenzanthracene; PYR: pyrene; TMPD: *N*,*N*,*N*′,*N*′-tetramethyl-*p*-phenylenediamine; Cp_2Ni: nickelocene; Cp^*_2Fe: decamethylferrocene.

Table 1 C_{60} complexes obtained and the data for their preparation

Entry	Complex	Method[a]	Solvent	Yield/%	Shape of the crystals	Ref.[b]
1	$BTX{\cdot}C_{60}{\cdot}CS_2$	1	CS_2	100	Rhombs	52, 53
2	$BTX{\cdot}C_{60}$	2	$C_2H_4Cl_2$, C_7H_8	70	Plates	52, 53
3	$(BA)_2C_{60}$	1	C_6H_6	60	Plates	
4	$(BXA)_2C_{60}$	1	C_7H_8	80	Needles	
5	$DAN{\cdot}C_{60}(C_6H_6)_3$	3	C_6H_6	100	Rhombs	54, 55
6	$TPC{\cdot}C_{60}$	1	C_6H_6	20	Pyramids	55
7	$TMT(C_{60})_3C_6H_6$	1	C_6H_6	90	Plates	
8	$(TMT)_2C_{60}(C_7H_8)_{0.5}$	1	C_7H_8	60	Parallelepipeds	
9	$(S_4N_4)_{1.33}C_{60}(C_6H_6)_{0.67}$	1	C_6H_6	90	Prisms	56
10	$S_4N_4{\cdot}C_{60}$	1	C_7H_8	60	Rhombs	56
11	$(BEDT\text{-}TTF)_2C_{60}(C_5H_5N)_2$	1	C_5H_5N	70	Plates	
12	$OMTTF{\cdot}C_{60}{\cdot}C_6H_6$	1	C_6H_6	90	Plates	23
13	$OMTTF{\cdot}C_{60}{\cdot}C_5H_5N$	1	C_5H_5N	70	Plates	
14	$(EDT\text{-}TTF)_2C_{60}{\cdot}CS_2$	1	CS_2	90	Plates	58
15	$EDT\text{-}TTF{\cdot}C_{60}{\cdot}C_6H_6$	1	C_6H_6	70	Needles	58
16	$(TMDTDM\text{-}TTF)_2C_{60}(CS_2)_3$	1	CS_2	30	Rhombs	57
17	$(BEDO\text{-}TTF)_2C_{60}$	1	CS_2	50	Prisms	
18	$BEDO\text{-}TTF{\cdot}C_{60}{\cdot}C_6H_6$	1	C_6H_6	50	Plates	
19	$DP\text{-}TTF{\cdot}C_{60}{\cdot}C_6H_6$	1	C_6H_6	50	Pyramids	
20	$(DMDP\text{-}TTF)_2C_{60}{\cdot}C_6H_6$	1	C_6H_6	50	Plates	
21	$OOT\text{-}TTF\ C_{60}{\cdot}C_7H_8$	2	C_6H_5Cl, C_6H_5CN	90	Needles	
22	$DBTTF{\cdot}C_{60}{\cdot}C_6H_6$	1	C_6H_6	70	Parallelepipeds	59
23	$DBTTF{\cdot}C_{60}{\cdot}C_5H_5N$	1	C_5H_5N	50	Plates	59
24	$TBT\text{-}TTF(C_{60})_2$	2	$C_2H_4Cl_2$, C_7H_8	40	Plates	
25	$EDY\text{-}BEDT\text{-}DT{\cdot}C_{60}{\cdot}C_6H_6$	1	C_6H_6	30	Needles	
26	$BNDY{\cdot}C_{60}$	1, 2	C_6H_6	80	Rhombs	
27	$TPDP(C_{60})_2(CS_2)_4$	1	CS_2	100	Parallelepipeds	60, 61
28	$DADTF(C_{60})_2CS_2$	1	CS_2	70	Plates	
29	$TBMA(C_{60})_2$	1	C_6H_6	80	Rhombs	
30	$TMPD{\cdot}C_{60}$	1	C_6H_5Cl	90	Prisms	16
31	$LCV{\cdot}C_{60}{\cdot}C_6H_5Cl$	1	C_6H_5Cl	50	Plates	
32	$BMPP{\cdot}C_{60}$	1	C_6H_6	90	Prisms	
33	$(TP)_2C_{60}$	1	C_6H_6	90	Parallelepipeds	
34	$PYR\sim C_{60}$	1	C_7H_8	90	Plates	
35	$TPB{\cdot}C_{60}$	1, 2	C_6H_6	100	Parallelepipeds	
36	$TPE{\cdot}C_{60}(C_6H_5Cl)_{0.5}$	1	C_6H_5Cl	80	Parallelepipeds	
37	$DPA{\cdot}C_{60}$	1	C_6H_6	70	Prisms	
38	$DBA{\cdot}C_{60}(C_6H_6)_3$	1	C_6H_6	80	Plates	
39	$(Cp^*_2Fe)_2C_{60}$	1	C_7H_8	70	Prisms	
40	$(Cp_2Ni)_xC_{60}(CS_2)_{1.8}$, $x<0.2$[c]	1	CS_2	10	Pyramids	
41	$CoTPP{\cdot}C_{60}(CS_2)_{0.5}$	1	CS_2	50	Parallelepipeds	62
42	$MnTPP(C_{60})_2(CS_2)_{1.5}$	1	CS_2	50	Parallelepipeds	62
43	$C_{60}(I_2)_{0.9}$	1	C_6H_6	50	Spherical	

[a]Methods of preparation: 1—evaporation of a solvent; 2—cooling of saturated solutions; 3—diffusion. [b]The literature data for the synthesis and some properties of the complexes. Elemental analysis, the AB of solvents in the IR spectrum, and the content of a solvent according to TG analysis for the complexes obtained are given as supplementary materials. [c]The complex was obtained by the evaporation of a CS_2 solution containing C_{60} and Cp_2Ni in a 1:2 molar ratio. The IR spectrum of the complex contains AB of C_{60}, CS_2 and additional weak AB which can be attributed Cp_2Ni^+. When an excess of nickelocene was used (1:10 molar ratio), the addition of Cp_2Ni to C_{60} proceeded with the precipitation of a brown powder with quantitative yield. The AB of the starting C_{60} are absent in the IR spectrum of the powder showing the formation of a novel chemical compound.[63]

breaking in complexes, and to attribute some C_{60} absorption bands in electronic absorption spectrum. The paper reports also the data on the syntheses, crystal structures, thermogravimetry, IR-, electronic, ESR-, X-ray photoelectron spectroscopies, and some physical-chemical properties of these compounds.

2 Experimental

2.1 General

IR spectra of the single crystals were registered with a Perkin Elmer 1725X spectrophotometer equipped with an IR microscope in the 650–3200 cm^{-1} range. The powdered samples pressed in KBr pellets (1:400) were measured in the 400–7000 cm^{-1} range. Electronic absorption spectra were registered with a Perkin Elmer Lambda 19 UV-VIS-NIR spectrophotometer in the 220–3000 nm range (KBr pellet, 1:2000). Electronic reflectance spectra of the single crystals were recorded with a microspectroreflectometer equipped with an UV-VIS microscope in the 240–1150 nm range. The spectra were recorded in polarised light at room temperature. The absorption spectra were derived from the reflectance ones by the Kramers–Kronig transformation.[51] Thermogravimetric analysis was carried out with a Q-1000 derivatograph in quartz bowls in the argon flow at a rate of heating 10–20 K min^{-1} in the 298–1273 K range. The temperature of loss of mass was determined from the minimum of DTG curve. X-Ray photoelectron (XP) spectra were measured with a VIEE-15 spectrometer. XP-Spectra were excited by Mg-Kα radiation ($h\nu = 1253.6$ eV) and calibrated as to the C1s peak (285.0 eV). ESR spectra were registered with a Radiopan SE/X 2547 spectrometer.

2.2 Preparation of C_{60} complexes

Fullerene of the 99% grade was used. Benzene and toluene were distilled over Na–benzophenone under argon. Chlorobenzene, 1,2-dichloroethane and CS_2 were distilled over P_2O_5. Pyridine was kept and distilled over KOH. The solvents were stored under argon.

Donor compounds used for the preparation of the C_{60} complexes and their abbreviations and names are presented in Fig. 1.

C_{60} complexes were prepared by three different methods. The preparation procedure is given for one complex; the other complexes were prepared analogously.

1 Slow evaporation of a solvent. $(TMT)_2C_{60}(C_7H_8)_{0.5}$ was prepared by the evaporation of toluene solution (25 mL) containing C_{60} (30 mg, 0.041 mmol) and TMT (35 mg, 0.082 mmol) during a week under argon. The crystals were washed with ether. The complex was formed as prisms of $2 \times 1 \times 1$ mm size in 60% yield (35 mg).

2 Cooling of saturated solutions. TBT-TTF$(C_{60})_2$ was prepared by mixing hot equimolar solutions of C_{60} (30 mg, 0.041 mmol) in toluene (25 mL) and TBT-TTF (31 mg, 0.041 mmol) in 1,2-dichloroethane (10 mL). The reaction mixture was evaporated to 1/3 of the initial volume. The resulted solution was cooled down to room temperature during 4 hours. The solvent was decanted and crystals were washed with ether. The complex was formed as plates in 60% yield (35 mg).

3 Diffusion method. DAN·$C_{60}(C_6H_6)_3$ was prepared by the mutual diffusion of benzene solutions of C_{60} (50 mg, 0.069 mmol in 50 mL of benzene) and DAN (30 mg, 0.083 mmol in 50 mL of benzene) in a U-shaped glass tube during 3 months. The crystals were washed with benzene. The complex was formed as rhombs of 2×2 mm size in quantitative yield.

The C_{60} complexes with Cp^*_2Fe, Cp_2Ni, MnTPP, and CoTPP, which are sensitive to oxygen, were prepared and stored under argon.

Table 1 shows the complexes obtained. All the complexes were characterised by elemental (C, H, N, and S), and thermogravimetric analyses and by IR- and XP-spectra.[52–62] Data which were not published previously are given as supplementary material.

Elemental analysis of the complexes usually shows a lower carbon content because of a large amount of carbon in the samples (80–99%). This is characteristic for fullerene containing compounds. In this case the composition of the complex was calculated from more precise values for S and N. Thermogravimetric analysis can yield a more precise value for the content (%) of the solvent in the complex. The IR-spectra allow identification of fullerene, donor, and solvent in the complexes. XP-spectra were used for the determination of a donor : fullerene stoichiometric ratio. It should be noted that if a sample contains CS_2, it is removed during the measurements and does not change the S : C atomic ratio.

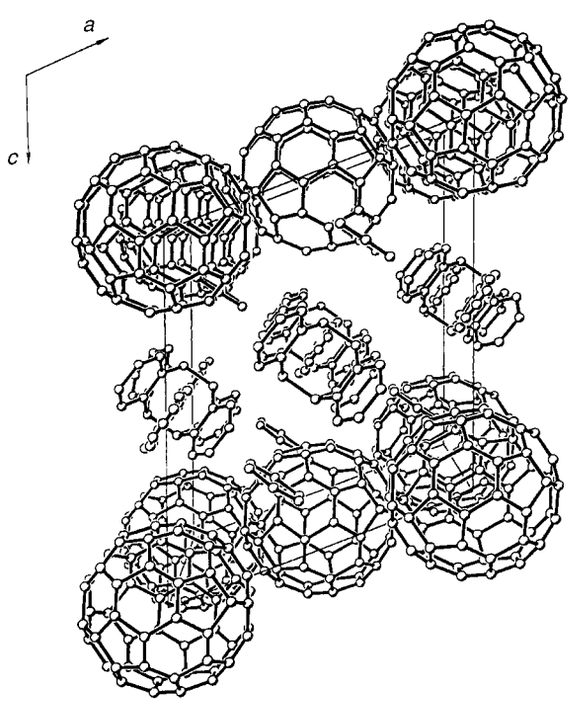

Fig. 2 Projection of the crystal structure of DAN·$C_{60}(C_6H_6)_3$ along the *ab* plane (Reprinted from Ref. 54, Copyright 1997, Royal Society of Chemistry).

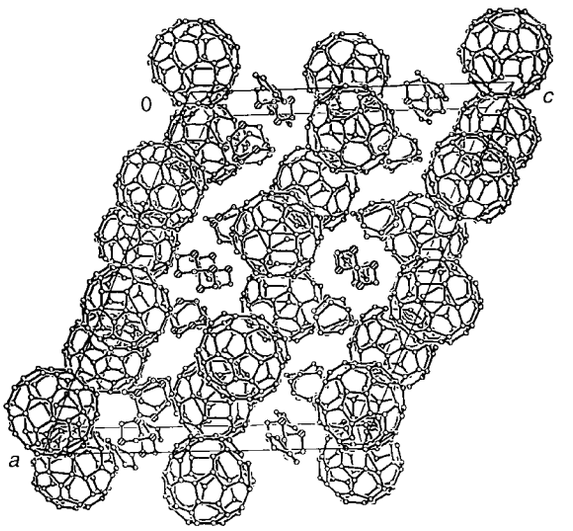

Fig. 3 Projection of the crystal structure of $(S_4N_4)_{1.33}C_{60}(C_6H_6)_{0.67}$ along the *ab* plane.[69]

3 Results and discussion

3.1 The formation of the C_{60} complexes

Most fullerene complexes are synthesised by a slow evaporation of a solvent. Two competing reactions can proceed:

$$C_{60}(\text{Solv.})_x + D \rightarrow C_{60}(\text{Solv.})_{x_1} \quad (1)$$

$$C_{60}(\text{Solv.})_x + D \rightarrow D_n(C_{60})_m(\text{Solv.})_k \quad (2)$$

where $x_1 < x$ in the solvate and $n = 1$–6, $m = 1$–3, $k = 0$–4 in the complex.

The solvates with solvents (Solv.) formed even on dissolution

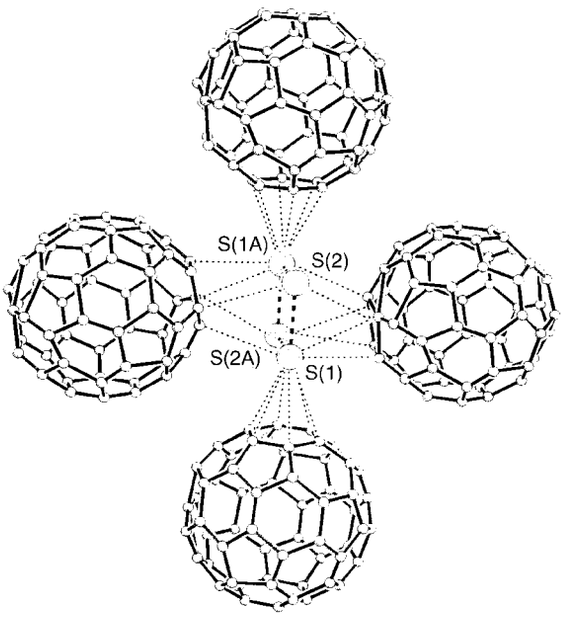

Fig. 4 Coordination of sulfur atoms of the central DBTTF fragment (S_4C_2) with C_{60} in the crystal structure of DBTTF·C_{60}·C_6H_6 (Reprinted from Ref. 59, Copyright 1997, Elsevier).

of fullerene.[64] The evaporation of the solvent in the presence of a donor yields either a solvate or a complex. In some cases the solvate can be isolated as crystals of the individual compound, for example, $C_{60}(C_6H_6)_4$,[65] $C_{60}(CS_2)_{0.4}$, and $C_{60}(C_5H_5N)_{0.4}$ (compounds obtained in this work).

We found:

a) In some cases formation of the complex is possible only at a certain donor : fullerene molar ratio, namely, 4 for TPC·C_{60}, 3.5 for DBTTF·C_{60}·C_6H_6, 4 for (DMDP-TTF)$_2C_{60}$·C_6H_6, and 6 for TBMA$(C_{60})_2$. Lower quantities of donors yield only C_{60} solvates.

b) Since complex formation proceeds in the presence of excess solvent relative to the donor, the yield of the complex can be increased by using a larger excess of donor relative to C_{60} (up to 20 : 1).

c) A specific feature of complex formation of fullerenes is a slow substitution of a solvent by a donor from a solvate shell of the fullerene molecule. For example, the evaporation of solvent for 4 hours yields only 2–5% of the TPDP$(C_{60})_2(CS_2)_4$ complex and the main product is $C_{60}(CS_2)_{0.4}$. Longer evaporation results in higher yields of the complex and a 20 days long evaporation results in an almost quantitative yield of the complex.[60]

Close sizes of donor and solvent molecules allow the formation of a continuous series of compounds. For example, the complex formation of S_4N_4 with C_{60} in benzene at different $S_4N_4 : C_{60}$ molar ratios yields the continuous series of compounds $(S_4N_4)_{2-x}C_{60}(C_6H_6)_x$, where $0.67 \leqslant x \leqslant 1.2$. We isolated the compounds with $x = 0.67$, 1.0, 1.1, 1.2 and different crystal shapes. Since both the size and the shape of C_6H_6 and S_4N_4 molecules are similar, a benzene molecule could substitute an S_4N_4 one in one of the positions of the crystal lattice. At high excess of S_4N_4, the probability of such substitution decreases and an $S_4N_4 : C_{60}$ molar ratio of more than 20 yields $(S_4N_4)_{1.33}C_{60}(C_6H_6)_{0.67}$ with a minimal benzene content. The toluene molecule cannot substitute S_4N_4. Therefore, the formation of only S_4N_4·C_{60} and $(S_4N_4)_2C_{60}$ is possible in toluene.[56]

3.2 The structures of the C_{60} complexes

Crystal structures have been determined for some complexes. All the complexes can be classified according to the packing of the C_{60} molecules in the crystal.

One-dimensional packing. The structure of BTX·C_{60}·CS_2 appears as chains of the C_{60} molecules packed along the $\bar{a}$ axis.[17] The distances between the centres of the C_{60} molecules

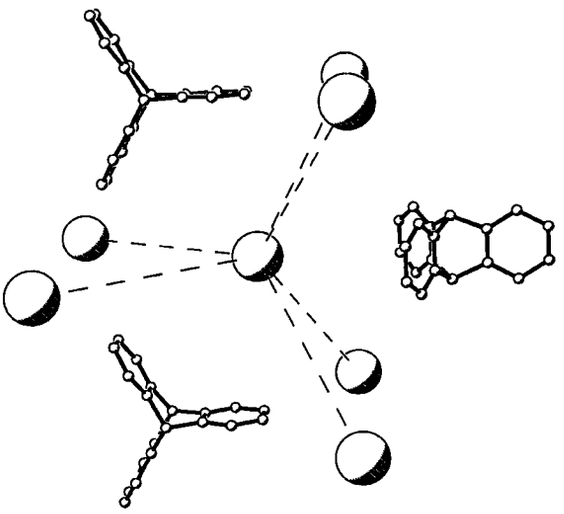

Fig. 5 The arrangement of C_{60} and TPC molecules in the crystal structure of TPC·C_{60}. The C_{60} molecules are marked by spheres.[55]

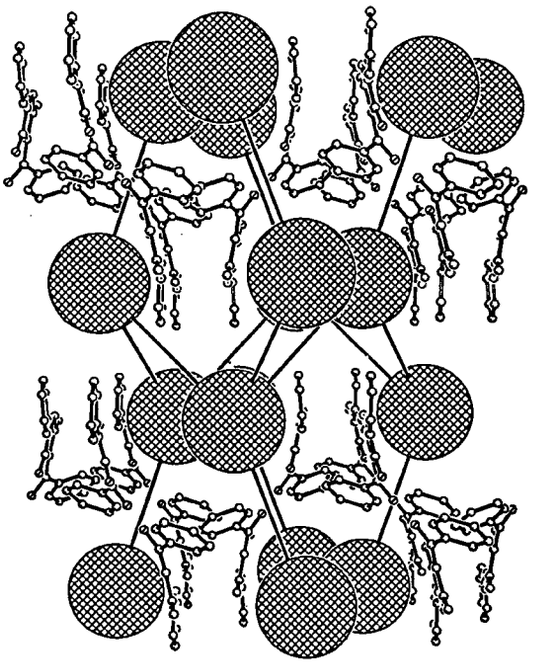

Fig. 6 The arrangement of C_{60} and BMPP molecules in the crystal structure of BMPP·C_{60}. The C_{60} molecules are marked by spheres.[71]

are 10.31 Å. Therefore, the C_{60} molecules are isolated from one another. The BTX molecules are coordinated to C_{60} by the phenylene groups and Te atoms. The Te···C(C_{60}) shortened contacts are within 3.64–3.85 Å. The CS_2 molecules have a number of shortened contacts (3.34–3.58 Å) with C_{60} as well. The conformation of the BTX molecule remains unchanged after coordination with C_{60}. A dihedral angle of 135.5° between the planes of the phenylene groups is close to that in the starting donor (138.8 and 140.5°).[66]

Layered packing. In TPDP$(C_{60})_2(CS_2)_4$ the layers comprising the C_{60} and CS_2 molecules alternate with the layers of TPDP along the $\bar{c}$ axis.[67]

The distances between the centres of the C_{60} molecules in the layers are 10.15 Å (170 K) and 10.20 Å (293 K), *i.e.* close to the van der Waals diameter of C_{60} (10.18 Å). The averaged lengths of the C–C bonds in C_{60} are 1.381(8) Å for 6 : 6 bonds and 1.451(6) Å for 6 : 5 bonds.

TPDP molecules are coordinated to the pentagonal and hexagonal faces of the C_{60} molecules by the phenyl groups. The central C=C bonds of the TPDP molecule in the complex are close to those in a neutral molecule, 1.384(9) and 1.385(8) Å, respectively.[68] However, the TPDP conformation in the complex strongly differs due to the rotation of phenyl rings relative to the plane of the dipyranylidene fragment.

In DAN·$C_{60}(C_6H_6)_3$, the layers of C_{60} molecules have distances between the centres equal to 10.08 Å, are parallel to the *ab* plane and alternate with the layers of DAN molecules (Fig. 2).[54] Each DAN molecule coordinates to two C_{60} molecules in the adjacent layers by the phenylene groups. The C(DAN)···C(C_{60}) distances are shortened and equal to ~3.4 Å. The conformation of the DAN molecule remains unchanged after coordination. Two benzene molecules are arranged in the C_{60} layer composed and one C_6H_6 molecule is arranged in the DAN layers.

In (TMDTDM-TTF)$_2C_{60}(CS_2)_3$ distorted hexagonal layers of C_{60} molecules alternate with layers of TMDTDM-TTF ones along the *ab* plane.[57] The closest distances between the centres of the C_{60} molecules along the *ab* diagonal are 10.09 Å. The asymmetric TMDTDM-TTF molecules are packed as "head-to-tail" dimers in the layers. The S···S distances are 3.7–3.8 Å inside the dimer and 3.84 Å between the dimers. Two of the

Table 2 Decomposition temperatures for C_{60} complexes

Entry	Complex	T_1/°C[a]	T_2/°C[a] (% loss of mass)	T_3/°C[a]
1	BTX·C_{60}	—	340 (11.6)	800
2	BNDY·C_{60}	—	390 (14.0)	730
3	$(BA)_2C_{60}$	—	300 (5.5), 480 (18.3)	750
4	S_4N_4·C_{60}	—	190 (8.3), 350 (8.4)	700
5	TPC·C_{60}	—	340 (21,7)	600
6	$(BXA)_2C_{60}$	—	375 (15,0)	700
7	TMPD·C_{60}	—	250 (12.6)	800
8	BMPP·C_{60}		360 (15,0)	600
9	$(TP)_2C_{60}$	—	420 (22,3)	720
10	PYR ~ C_{60}	—	360 (1,5)	800
11	TPB·C_{60}	—	300 (17.7)	700
12	DPA·C_{60}		450 (16,8)	700
13	$(Cp^*_2Fe)_2C_{60}$	—	330 (37,2)	800
14	I_2·C_{60}	—	180 (21.8)	720
15	$(BEDT\text{-}TTF)_2C_{60}(C_5H_5N)_2$	240	250 (19.2)[b]	700
16	BEDO-TTF·C_{60}·C_6H_6	150	240 (15.5)	800
17	DAN·$C_{60}(C_6H_6)_3$	150	330 (27.2)	800
18	DBTTF·C_{60}·C_6H_6	130	430 (16.7)	800
19	OMTTF·C_{60}·C_6H_6	120	290 (21.6)	800
20	$TMT(C_{60})_3C_6H_6$	170	400 (9.1)	800
21	$(S_4N_4)_{0.9}C_{60}(C_6H_6)_{1.1}$	80, 130	170 (7.2), 330 (5.6)	630
22	$(TMT)_2C_{60}(C_7H_8)_{0.5}$	191	393 (23.0)	800
23	$(TMDTDM\text{-}TTF)_2C_{60}(CS_2)_3$	80	265 (15.2)	665
24	$(EDT\text{-}TTF)_2C_{60}$·CS_2	110	290 (11.8)	700
25	$TPDP(C_{60})_2(CS_2)_4$	130	540 (5.6)	640
26	BTX·C_{60}·CS_2	210	340 (9.8)	800
27	TPE·$C_{60}(C_6H_5Cl)_{0.5}$	140	370 (26,5)	600
28	OOT-$TTFC_{60}$·C_7H_8	190	300 (24,5)	750
29	CoTPP·$C_{60}(CS_2)_{0.5}$	180	490 (7,3)	800
30	LCV·C_{60}·C_6H_5Cl	150	350 (4.7)	700

[a] T_1: temperature of solvent removal; T_2: of donor decomposition; T_3: of fullerene sublimation. [b] Two peaks overlapping; a total loss of mass is given in brackets.

three CS_2 molecules are arranged in the fullerene layer and one CS_2 molecule in the donor layer.

In $(S_4N_4)_{1.33}C_{60}(C_6H_6)_{0.66}$ the C_{60} molecules form dense distorted hexagonal layers (Fig. 3).[56,69] Each fullerene molecule has eight shortened $C_{60}\cdots C_{60}$ contacts, six contacts are inside the layer and two are between the layers. The closest distances between the centres of the C_{60} molecules are 9.87–10.08 Å. The S_4N_4 and C_6H_6 molecules occupy cavities in the interlayer space and are positioned at the vertices of regular hexagons relative to the C_{60} molecules. The ordered S_4N_4 molecules occupy one position and the disordered S_4N_4 and C_6H_6 ones occupy another position. The bond lengths and valence angles of the ordered S_4N_4 molecules in the complex remain almost unchanged with respect to the starting S_4N_4.[70]

Three-dimensional arrangement of C_{60} molecules. In DBTTF·C_{60}·C_6H_6 the packing of C_{60} molecules is close to simple cubic packing.[59] Each fullerene molecule is surrounded by six adjacent C_{60}s, which form a distorted octahedron with

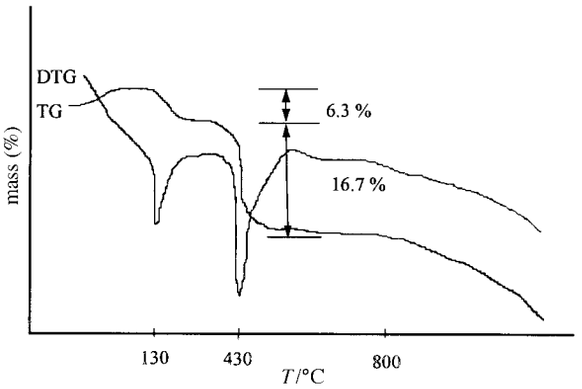

Fig. 7 Thermograviagram of the DBTTF·C_{60}·C_6H_6 decomposition under argon. The heating rate is 10 °C min^{-1}.

the distances between the centres equal to 10.4 Å along the $\bar{c}$ axis and equal to 10.5 Å in the *ab* plane. These distances are essentially greater than the van der Waals diameter of C_{60} (10.18 Å). Therefore, the C_{60} molecules are isolated from one another.

The DBTTF molecules form chains along the $\bar{c}$ axis. Each DBTTF molecule has shortened S(DBTTF)$\cdots$C(C_{60}) contacts with the four fullerene molecules (Fig. 4). Two S atoms (S1 and S1A) of the central S_4C_2 fragment are coordinated to the centre of the hexagonal face of the two C_{60} molecules (1 and 4). The S(DBTTF)$\cdots$C(C_{60}) distances are 3.47–3.72 Å. The plane of the central S_4C_2 fragment is perpendicular to the plane of these hexagonal faces indicating the n–π interaction.

The central S_4C_2 fragment of the DBTTF molecule is almost parallel (the dihedral angle is 10.8°) to the hexagonal face of the two other C_{60} molecules (2 and 3). An almost parallel arrangement of these fragments indicates the π–π interaction. The efficient packing of DBTTF and C_{60} molecules is attained by distortion of the flat DBTTF molecule. The dihedral angles between the central S_4C_2 fragment and the outer planes are 25.5°.

Each benzene molecule coordinates to two C_{60} ones occupying the cavities in the fullerene framework.

In TPC·C_{60} each C_{60} molecule is surrounded by six adjacent ones (Fig. 5).[55] The distances between the centres are 10.17 Å, *i.e.* close to the van der Waals diameter of C_{60} (10.18 Å). The shape of the TPC molecule enables its efficient coordination to three fullerene ones by means of the phenylene groups. The C_{60} molecules are arranged in the vertices of an equilateral triangle whose centre is occupied by the TPC molecule.

In BMPP·C_{60} each C_{60} molecule is also surrounded by adjacent ones (Fig. 6).[71] The distances between the centres of the C_{60} molecules are 9.988–10.154 Å. Each BMPP molecule coordinates to two C_{60} ones by the nitrogen atoms (the N(BMPP)$\cdots$C(C_{60}) distances are 3.18–3.41 Å), and by the benzoyl group (the C(BMPP)$\cdots$C(C_{60}) distances are 3.43–3.79 Å). The conformation of the BMPP molecule in the

Table 3 Position of the $F_{1u}(4)$ mode of C_{60} in the complexes at room temperature, the shift of the AB with respect to the starting C_{60}, the degree of charge transfer (δ) estimated from eqn. (1)

Entry	Complex	$F_{1u}(4)$ mode/cm^{-1}	Shift/cm^{-1}	δ
	C_{60}	1429[79]	—	—
1	TMPD·C_{60}	1426	3	0.09
2	BTX·C_{60}	1427	2	<0.06
3	(EDT-TTF)$_2C_{60}$·CS_2	1427	2	<0.06
4	OMTTF·C_{60}·C_6H_6	1428	1	<0.03
5	OMTTF·C_{60}·C_5H_5N	1428	1	<0.03
6	TPDP$(C_{60})_2(CS_2)_4$	1428	1	<0.03
7	DTDAF$(C_{60})_2CS_2$	1428	1	<0.03
8	EDY-BEDT-DT·C_{60}·C_6H_6	1428	1	<0.03
9	EDT-TTF·C_{60}·C_6H_6	1428	1	<0.03
10	TMT$(C_{60})_3C_6H_6$	1428	1	<0.03
11	CoTPP·$C_{60}(CS_2)_{0.5}$	1428	1	<0.03
12	OOT-TTFC_{60}·C_7H_8	1428	1	<0.03
13	$(Cp_2Ni)_xC_{60}(CS_2)_2$, $x<0.2$	1428	1	<0.03
14	S_4N_4·C_{60}	1429	0	0
15	BNDY·C_{60}	1429	0	0
16	$(S_4N_4)_{0.9}C_{60}(C_6H_6)_{1.1}$	1430	0	0
17	TPC·C_{60}	1425, 1431[a]	—	—
18	$(Cp^*_2Fe)_2C_{60}$	1425, 1432[a]	—	—
19	DAN·$C_{60}(C_6H_6)_3$	1426, 1430[a]	—	—
20	BTX·C_{60}·CS_2	1428, 1432[a]	—	—

[a]The splitting of the $F_{1u}(4)$ mode of C_{60} on freezing the rotation of the C_{60} molecules.

complex is more planar than in the starting molecule. The values of the rotation angles of the phenyl and benzoyl groups about the pyrazolone ring decrease to 15.0 and 57.5°, respectively, as compared to 28.3 and 59.9° in the starting BMPP.

Therefore, the C_{60} complexes exhibit a wide variety of crystal packings ranging from one-dimensional chains to three-dimensional skeleton structures composed of C_{60} molecules. The type of packing of the C_{60} molecules in the crystal and the distances between them are to a great extent defined by the size and conformation of the donor and solvent molecules used. However it is rather difficult to predict the crystal structure of C_{60} molecular complexes from only the size and shape of the donor molecule. As one should expect, the decrease of linear sizes of the donor component results in shorter distances between the C_{60} molecules in the crystals of the complexes. For example, on substitution of the large TPDP molecule for smaller linear TMDTDM-TTF, DAN, and S_4N_4 ones, the distances between the C_{60} molecules in the layer decrease from 10.20 down to 9.87 Å, respectively. The application of donor molecules (DAN, TMDTDM-TTF dimer, TPDP, and S_4N_4) capable of coordinating only two C_{60} molecules arranged above and under the donor molecule results in the formation of predominantly layered structures, while the application of donor molecules capable of coordinating three (TPC) or four (DBTTF and BTX) fullerene molecules results in the formation of three-dimensional structures in which one could distinguish the chains of the C_{60} molecules as, for example, in the case of the BTX·C_{60}·CS_2 complex.

3.3 Thermogravimetry of fullerene complexes

Thermal stability of most of the fullerene complexes was studied by thermogravimetric (TG) analysis (Table 2).

One could usually observe three temperature ranges, in which the loss of the sample mass takes place (Fig. 7). The first temperature range is associated with the removal of a solvent, then partial or full decomposition of the donor is observed, and further temperature increase leads to fullerene sublimation.

Solvent removal from the C_{60} complexes containing solvents is realised in different temperature ranges. Thus carbon disulfide (bp = 46 °C) is removed from the complexes at 80–210°C; benzene (bp = 81 °C) at 80–170 °C; toluene (bp = 111 °C) at 190 °C; chlorobenzene (bp = 132 °C) at 140–150 °C, and pyridine (bp = 115 °C) beginning from 240 °C.

The temperature of solvent removal seems to be affected by

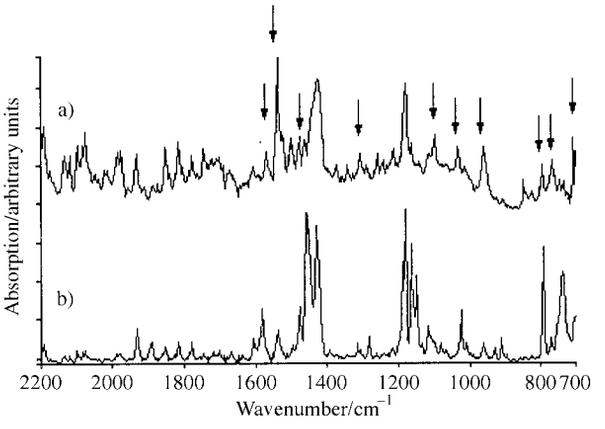

Fig. 8 IR spectra of the $(I_2)_{0.9}C_{60}$ (a) and TPC·C_{60} (b) single crystals. The most intense AB of symmetry-forbidden vibrations of C_{60} are marked by arrows.

the strength of binding in the complex. Thus the CS_2 molecules have no shortened contacts with C_{60} in (TMDTDM-TTF)$_2C_{60}(CS_2)_3$[57] and the removal of the solvent starts at as low as 80 °C. In BTX·C_{60}·CS_2, which has shortened contacts between CS_2 and C_{60}, the removal of the solvent starts only at 210 °C.

The values of decomposition temperatures are commonly close for the uncomplexed donors and the donors involved in the complexes. In some cases the temperatures of donor decomposition increase by 10 °C, for example, in BTX·C_{60}·CS_2 and S_4N_4·C_{60}. In C_{60} complexes with tetramethoxythianthrene, $(TMT)_2C_{60}(C_7H_8)_{0.5}$ and TMT$(C_{60})_3(C_6H_6)$, a decrease in the temperature of donor decomposition by 20–30 °C as compared to the starting donor is observed. The strongest changes for donor decomposition are observed in TPDP$(C_{60})_2(CS_2)_4$. The starting TPDP is decomposed in two temperature ranges, namely, at 400 °C (27.1%) and 530 °C (28.2%). In the complex, a partial decomposition of the donor is observed only at 540 °C (5.8%).

The temperature of fullerene sublimation coincides for most complexes with that for pure C_{60} (800 °C).[72] However, for some complexes the temperature of fullerene sublimation is essentially lower, namely, 665 °C for (TMDTDM-TTF)$_2C_{60}(CS_2)_3$, 640 °C for TPDP$(C_{60})_2(CS_2)_4$, 600 °C for BMPP·C_{60}, 630 °C

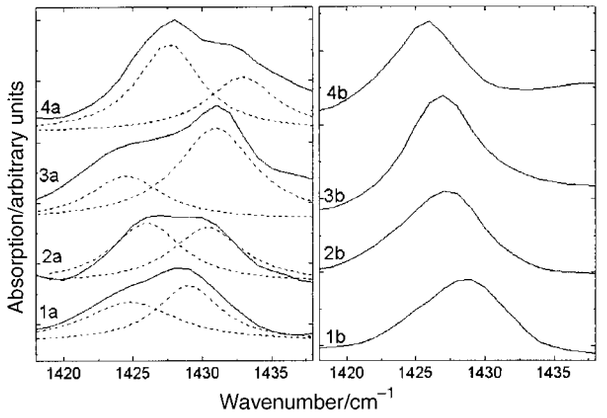

Fig. 9 IR spectra of single crystals of the complexes at 1420–1440 cm^{-1} (T=300 K): (1a) $(Cp^*_2Fe)_2C_{60}$; (2a) $DAN{\cdot}C_{60}{\cdot}(C_6H_6)_3$; (3a) $TPC{\cdot}C_{60}$; (4a) $BTX{\cdot}C_{60}{\cdot}CS_2$; (1b) $BNDY{\cdot}C_{60}$; (2b) $(EDT\text{-}TTF)_2C_{60}{\cdot}CS_2$; (3b) $BTX{\cdot}C_{60}$; (4b) $TMPD{\cdot}C_{60}$.

for $(S_4N_4)_{0.9}C_{60}(C_6H_6)_{1.1}$. The removal of a large amount of CS_2 or donor decomposition accompanied by nitrogen evolution seems to loosen the crystal structure of the complex, thus breaking the bonds between fullerene molecules and lowering its sublimation temperature.

3.4 IR Spectroscopy of fullerene complexes

IR spectroscopy was used for the studies of both single crystals and pressed pellets of C_{60} complexes.[73–75] At the formation of the complex, the redistribution of electron density on donor and fullerene molecules and the lowering of the symmetry of C_{60} environment can be observed. These changes are reflected in IR spectra. It is shown[76,77] that the $F_{1u}(4)$ C_{60} mode at 1429 cm^{-1} is the most sensitive to the changes in charge and symmetry of the C_{60} environment. Therefore, we analysed the changes in this mode. The absorption bands (AB) of other IR active modes of C_{60} (527, 577, and 1183 cm^{-1}) are shifted by less than $\pm$1 cm^{-1} on complex formation. The accuracy of 1 cm^{-1} does not exceed spectral resolution of IR spectrometers used in experiments.

3.4.1 Evaluation of degree of charge transfer. The degree of charge transfer (δ) is the main characteristic, which defines many physical properties including magnetic and conducting ones.

The dependency of the position of $F_{1u}(4)$ mode on the charge of the C_{60} molecule is almost linear.[76] This linear dependency allowed us to derive the expression to evaluate δ from the shift of this mode: $\delta \cong 0.03\Delta\nu$ (1), where $\Delta\nu$ is the difference in wavenumbers for the $F_{1u}(4)$ mode in starting C_{60} (1429 cm^{-1}) and the corresponding complex.[73,78]

It should be noted that this equation is valid only for the C_{60} complexes in which the $F_{1u}(4)$ mode is not split and does not coincide with the AB of solvents and donors.

Both experimental error ($\pm$1 cm^{-1}) and the effect of the crystalline field determine the accuracy of the determination of the δ value. The position of the $F_{1u}(4)$ mode is within $\pm$2.5 cm^{-1} for mono anion-radical salts of $C_{60}^{-\cdot}$ (δ=1) with different crystal structures.[78] Therefore, the accuracy of this method is not higher than $\pm$0.08, and small shifts of $F_{1u}(4)$ mode ($\leqslant$2.5 cm^{-1}) can be caused by the effect of crystalline field rather than by charge transfer.

It is seen from Table 3 that the shifts of $F_{1u}(4)$ mode in the complexes are within the accuracy of this method ($\pm$2 cm^{-1}) and these compounds may be considered as neutral complexes ($\delta \leqslant 0.06$). For $TMPD{\cdot}C_{60}$ the shift of this mode is equal to 3 cm^{-1} and it could be attributed to the complex with a weak charge transfer.

Table 4 Maxima of AB in electronic absorption spectra of the starting donors and the donors in the complexes

Donor	λ/nm	Complex	λ/nm
BA	415	$(BA)_2C_{60}$	408
EDY-BEDT-DT	454	$EDY\text{-}BEDT\text{-}DT{\cdot}C_{60}{\cdot}C_6H_6$	444
TPDP	463	$TPDP(C_{60})_2(CS_2)_4$	462
CoTPP	429	$CoTPP{\cdot}C_{60}(CS_2)_{0.5}$	433

3.4.2 Changes in IR spectra of donors. Complex formation is evident in the shifts of some donor AB (up to 8 cm^{-1}) and redistribution of their intensity in the IR spectra of the complexes relative to the starting donors. This is associated first of all with significant changes in the conformation of the donor molecules on coordination to a spherical C_{60} molecule.

The frequency corresponding to characteristic vibrations of the central C=C bond of substituted tetrathiafulvalenes and dipyranylidenes is the most sensitive to the changes in electron density on donor molecules.[79] In $TPDP(C_{60})_2(CS_2)_4$ and $DADTF(C_{60})_2CS_2$ the small shifts (2–3 cm^{-1}) of the AB of the vibration of the C=C bond to higher frequencies is observed, while in $TBT(C_{60})_2$ and $(BA)_2C_{60}$ its position remains almost unchanged.

It should especially be noted that there is an increase of intensity and significant low-frequency shifts (up to 5–10 cm^{-1}) of the AB of corresponding C–H vibrations of phenyl and phenylene groups of the TPDP, TPC, DAN, and BTX by which they are coordinated to the C_{60} molecule.[54,78]

3.4.3 Manifestation of symmetry-forbidden vibrations of C_{60}. The C_{60} molecule is known to possess I_h symmetry[2] and the C_{60} spectrum (in the KBr matrix) shows only four symmetry-allowed IR-active $F_{1u}(1–4)$ modes. The IR transmission spectra of C_{60} single crystals are more complicated[80] and show about 180 additional weak AB. The additional AB at wave numbers $<$1600 cm^{-1} are assigned to the symmetry-forbidden vibrations of C_{60} and at wave numbers $>$1600 cm^{-1} to the combination vibrations and the overtones.[76,80] The appearance of the symmetry-forbidden vibrations (for the I_h group) is explained by the breaking of symmetry of the C_{60} environment due to the interaction of the adjacent C_{60} molecules, dislocations, and impurities in the crystal.[80]

In the complexes of nonstoichiometric composition, the breaking of symmetry is possible because of an irregular arrangement of donor and solvent molecules in the crystal structures of the complexes. This results in the appearance of intense AB of symmetry-forbidden vibrations, for example, in the spectrum of the $(I_2)_{0.9}C_{60}$ single crystals (Fig. 8a). All AB are attributed to C_{60}, since the AB of iodine are observed at

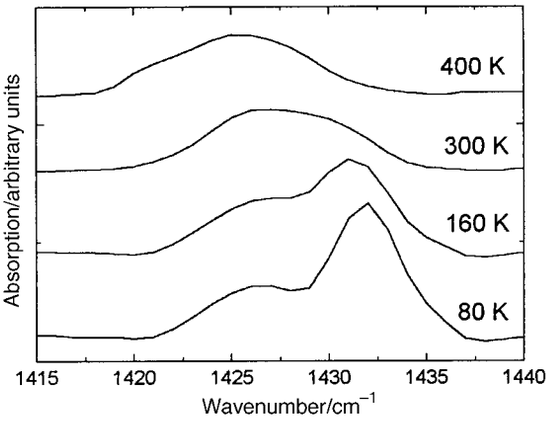

Fig. 10 Splitting of the $F_{1u}(4)$ mode of C_{60} into two components in $DAN{\cdot}C_{60}(C_6H_6)_3$ with the temperature decrease.

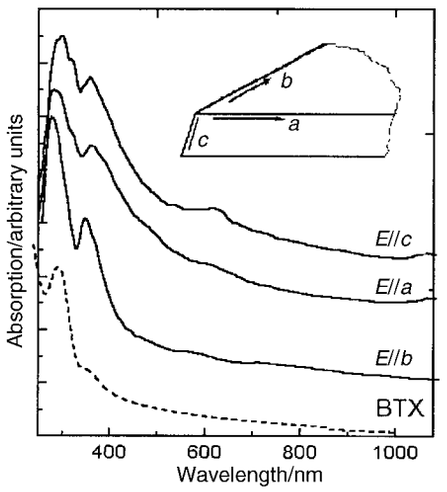

Fig. 11 Polarised absorption spectra of the BTX·C_{60}·CS_2 single crystals measured along the *a*, *b*, and *c* axes and the absorption spectrum of BTX in a KBr matrix (Reprinted from Ref. 83, Copyright 1998, Elsevier).

$<400\ cm^{-1}$ and the AB characteristic of benzene, which was used as a solvent, are absent. The AB at 712, 769, 795, 962, 1035, 1100, 1117, 1343, 1478, 1539, and 1580 cm^{-1} can be attributed to symmetry-forbidden vibrations of C_{60}. The most intense ones are marked by arrows. The positions of these bands in the spectrum of $(I_2)_{0.9}C_{60}$ are close to those in the spectrum of C_{60} single crystals.[80] At wavenumbers $>1600\ cm^{-1}$, one observes the combination vibrations and the overtones analogous to those in the C_{60} spectrum.[76]

Most fullerene molecular complexes have a stoichiometric composition and a regular crystal lattice with ordered donor and solvent molecules. The symmetry of the C_{60} environment in these complexes is higher than in non-stoichiometric ones and the intensity of symmetry-forbidden modes is essentially lower, as for example, in the IR spectrum of TPC·C_{60} single crystals (Fig. 8b).

3.4.4 Splitting of $F_{1u}(4)$ mode of C_{60} in molecular complexes. Interesting features were observed in the IR spectra of single crystals of the complexes. It is known[81] that the spectrum of C_{60} single crystals shows an unsplit $F_{1u}(4)$ mode at room temperature, whose halfwidth is 4 cm^{-1}. Decreasing the temperature below that of the orientational phase transition (255 K) in the C_{60} crystals results in the splitting of this mode into three components. As this takes place, the $F_{1u}(3)$ mode remains unsplit.[81]

The room-temperature spectra of the C_{60} complexes differ somewhat from that of C_{60}.[74] Fig. 9 presents the $F_{1u}(4)$ mode of C_{60} in complexes. The donor molecules do not absorb noticeably in this range.

For the first group of the complexes (Fig. 9 (1a–4a)), the $F_{1u}(4)$ mode is split into two components and can be presented as a sum of the two Lorentzian contours with equal linewidths of $\sim 6\ cm^{-1}$ (Table 4). The splitting of the $F_{1u}(3)$ mode at 1183 cm^{-1} is not observed in complexes or in the C_{60} crystals.

The F_{1u} C_{60} modes are threefold degenerate,[2] therefore their splitting indicates the lowering of symmetry of the C_{60} environment. The presence of only two components for the threefold degenerate mode can be attributed to a large halfwidth ($\sim 6\ cm^{-1}$) of the components and a relatively low resolution of the instrument (2 cm^{-1}).

There are several causes for the lowering of the symmetry of the C_{60} environment.

One of them is the changes in the local crystalline field. At the orientational phase transition in the C_{60} crystals, the free rotation of the C_{60} molecules at room temperature becomes a

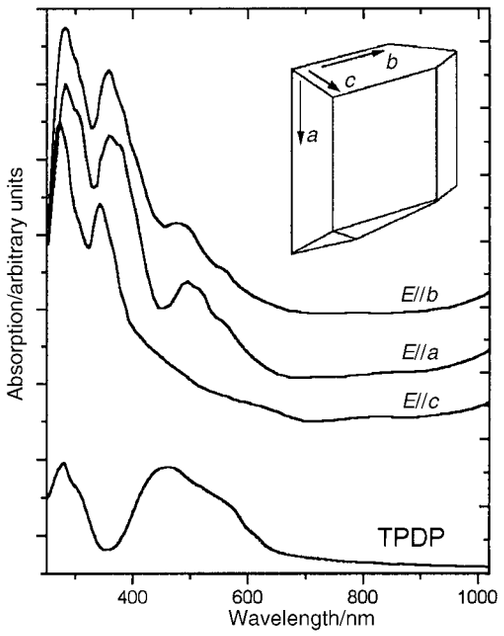

Fig. 12 Polarised absorption spectra of the TPDP$(C_{60})_2(CS_2)_4$ single crystals measured along the *a*, *b*, and *c* axes and the absorption spectrum of TPDP in a KBr matrix.

ratchet rotation when the electron-rich 6–6 bonds are located above the electron-deficient centres of pentagonal or hexagonal faces of C_{60}. Such changes in the local crystalline field provide the splitting of the $F_{1u}(4)$ mode with the retention of the unsplit $F_{1u}(3)$ mode.[81]

Similarly, changes in the local crystalline field in complexes can be caused by the transition from free to ratchet rotation of the C_{60} molecules. In this case the electron-rich groups of the donors can be located above the electron-deficient centres of C_{60}.

The other cause can be the lowering of position symmetry of C_{60}. The orientational phase transition in the C_{60} crystals is accompanied by the change from a face-centred cubic (fcc) lattice to a simple cubic one and the lowering of position symmetry of the C_{60} molecules from T_h symmetry to S_6.[76]

The position symmetry of the C_{60} molecules in the complexes with tetragonal, hexagonal, rhombic, and monoclinic lattice is lower than in the fcc lattice of C_{60}. This can result in the splitting of F_{1u} modes in the complexes at the freezing of free rotation of the C_{60} molecules. However, in this case the splitting of the $F_{1u}(3)$ mode with the same symmetry as the $F_{1u}(4)$ mode is beyond the resolution of the experiment.

In both cases the splitting of $F_{1u}(4)$ mode is observed only at

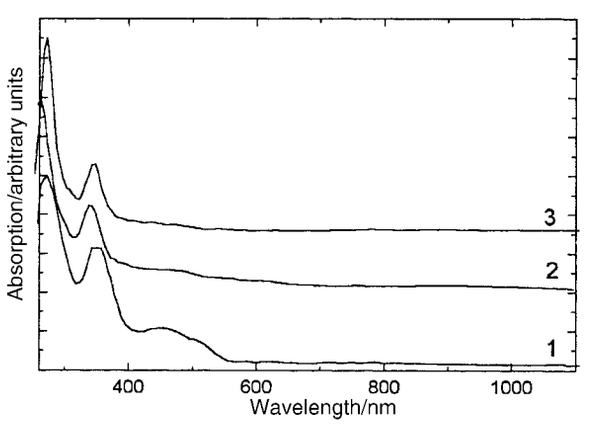

Fig. 13 Absorption spectra of the starting C_{60} (1), DBTTF·C_{60}·C_6H_6 (2), and TPC·C_{60} (3) single crystals (Reprinted from Ref. 83, Copyright 1998, Elsevier).

the freezing of the C_{60} rotation. In contrast to the C_{60} crystals, in which the adjacent fullerene molecules interact, the freezing of rotation in the complexes proceeds due to the interaction of C_{60} with the donor and solvent molecules.

According to the IR spectra, the rotation of the C_{60} molecules is frozen even at room temperature in the complexes with DAN, TPC, Cp^*_2Fe, and BTX. This is associated with the steric complementarity of the shapes of these donor molecules to the spherical C_{60} ones, which results in the formation of multiple van der Waals contacts. Solvent molecules can make an additional contribution. In fact, according to the X-ray data the solvent and fullerene molecules have shortened van der Waals $C(C_{60})\cdots S(CS_2)$ contacts in $BTX\cdot C_{60}\cdot CS_2$.[17] These shortened contacts seems to define the freezing of the rotation of the C_{60} molecules, since in $BTX\cdot C_{60}$ the $F_{1u}(4)$ mode remains unsplit (Fig. 11.3b). The absence of free rotation of the C_{60} in $BTX\cdot C_{60}\cdot CS_2$ and $DAN\cdot C_{60}(C_6H_6)_3$ at room temperature is confirmed also by the X-ray data.[17,54]

For the second group of the complexes (Fig. 9(1b–4b)), the $F_{1u}(4)$ mode with a halfwidth of $\sim 6\ cm^{-1}$ is not split at room temperature indicating free rotation of C_{60}.

We found orientational transitions in some complexes and solvates of C_{60} at lower and elevated temperatures similar to the phase transition in C_{60} at 255 K.[75]

In $DAN\cdot C_{60}(C_6H_6)_3$ the $F_{1u}(4)$ mode is split at room temperature to two components with the maxima at 1426 and $1430\ cm^{-1}$ (Fig. 10). At 80 K two components of the $F_{1u}(4)$ mode are well pronounced. On heating above 310 K, the splitting of the $F_{1u}(4)$ mode is eliminated and its AB becomes single with the maximum at $1427\ cm^{-1}$. It seems that the orientational transition is realised in the complex near this temperature after which the rotation of the C_{60} molecules becomes free.

In $BNDY\cdot C_{60}$ and $C_{60}(CS_2)_{0.4}$, the $F_{1u}(4)$ mode remains unsplit at elevated temperatures (up to 350 K). However, splitting of this mode is observed on decreasing the temperature down to 300 and 250 K, respectively.[75]

In $TPC\cdot C_{60}$ and $BTX\cdot C_{60}\cdot CS_2$, the splitting of the $F_{1u}(4)$ mode which is observed at room temperature is not eliminated on heating up to 370 K.

The splitting of the $F_{1u}(4)$ mode in the C_{60} complexes indicates the orientational transition attributed to the freezing of the C_{60} rotation. The temperature of this transition allows the estimation of the degree of donor–C_{60} interaction. Such an interaction is most strongly pronounced in the C_{60} complexes of donors possesssing certain molecular shapes. The shape must correspond sterically to the spherical surface of the C_{60} molecule (TPC, BTX, and DAN).

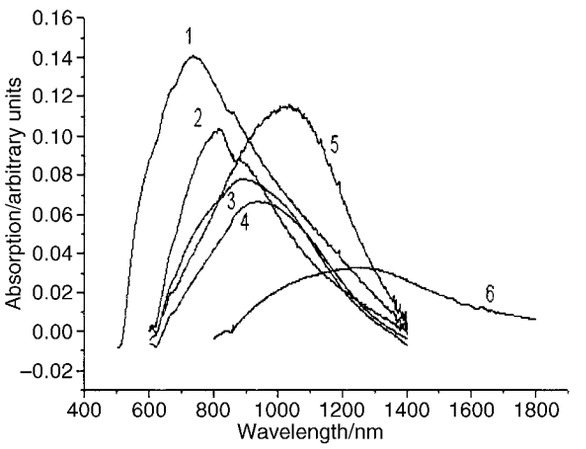

Fig. 14 Charge transfer bands of the C_{60} complexes in the solid state in the 500–1600 nm range:[84] (1) $DBTTF\cdot C_{60}\cdot C_6H_6$; (2) $(BEDT\text{-}TTF)_2C_{60}(Py)_2$; (3) $(EDT\text{-}TTF)_2C_{60}\cdot CS_2$; (4) $(DMDP\text{-}TTF)_2C_{60}\cdot C_6H_6$; (5) $OMTTF\cdot C_{60}\cdot C_6H_6$; (6) $TPDP(C_{60})_2(CS_2)_4$.

3.5 Electronic spectra

The electronic states of the donors and fullerenes and the intermolecular electron transfer in the complexes were studied by electronic spectroscopy.[82–84] The features of the absorption spectra of the C_{60} complexes are considered for one example but this is characteristic for all the C_{60} complexes.

Fig. 11 represents the absorption spectrum of the $BTX\cdot C_{60}\cdot CS_2$ single crystals in three different polarisations of light with respect to the crystal faces.

The position of the AB at 340 and 260 nm (± 5 nm) attributed to symmetry-allowed electronic transitions in C_{60} remains unchanged with respect to the starting C_{60}. A weak donor–C_{60} interaction does not affect these transitions significantly.[82,83]

The AB of the donors in the UV range (220–400 nm) are less intense than those of C_{60} and appear as a shoulder or are not observed at all. For example, the AB of BTX is pronounced as a shoulder in *a* and *c* polarisations in the spectrum of $BTX\cdot C_{60}\cdot CS_2$.

The intensity of the AB of C_{60} at 400–600 nm is relatively low in the spectra of the complexes and AB of the donors can be observed in this range. Sometimes donor AB are shifted up to 11 nm with respect to those of the starting ones (Table 4).

In contrast to the isotropic AB of C_{60}, the AB of the donors are polarised in the crystal. For example, in $TPDP(C_{60})_2(CS_2)_4$, the AB of TPDP with the maximum at 463 nm is pronounced only in *a* and *b* polarisations (Fig. 12). The X-ray data show that the layers of TPDP molecules are arranged in the *ab* plane in this complex.

The main changes in the spectra of the complexes are associated with the changes in intensity of the C_{60} absorption in the 420–530 nm range[83] and the appearance of new weak AB at 620–1240 nm attributed to intermolecular electron transfer from the donor to fullerene molecules.[83,84]

In $BTX\cdot C_{60}\cdot CS_2$ a new weak AB at 625 nm (1.98 eV) is pronounced in *c* polarisation (Fig. 11). The dependence of the intensity of this band on polarisation and its absence in the spectra of the starting C_{60} and BTX allow this band to be attributed to a charge transfer band (CTB). The position of this band is also close to the position of symmetry-forbidden HOMO–LUMO transitions of C_{60}. Therefore, this band can alternatively be attributed to C_{60}. The increase in intensity of this band relative to starting C_{60} may be associated with the breaking of C_{60} symmetry on coordination with the BTX molecule. However in this case we must assume that the symmetry-forbidden HOMO–LUMO transitions of C_{60} are polarised in $BTX\cdot C_{60}\cdot CS_2$.

3.5.1 Changes in intensity of the C_{60} absorption in the 420–530 nm range. Fig. 11 and 13 demonstrate the absorption spectra of the $BTX\cdot C_{60}\cdot CS_2$ (R_1 polarisation), $DBTTF\cdot C_{60}\cdot C_6H_6$, and $TPC\cdot C_{60}$ single crystals. It is seen that the absorption of C_{60} at 420–530 nm is less intense in the complexes than in the C_{60} crystals (Fig. 13.1). Absorption of donors is absent in this spectral range.

The nature of the C_{60} absorption at 420–530 nm in not clear. It is attributed to the symmetry-forbidden HOMO–LUMO transition in one C_{60} molecule[85,86] and to intermolecular HOMO–LUMO electron transfer between adjacent C_{60} molecules.[87,88] In the latter case the intensity of these transitions depends on the distances between the C_{60} molecules.

The distances between the C_{60} molecules in the complexes are larger than those in C_{60}, since donor and solvent molecules are arranged between them. The closest distance between the centres of the C_{60} molecules is 10.02 Å in the C_{60} crystals[89] and in $BTX\cdot C_{60}\cdot CS_2$, $DBTTF\cdot C_{60}\cdot C_6H_6$, and $TPC\cdot C_{60}$ it is equal to 10.40, 10.31, and 10.17 Å, respectively.[17,59,55] These distances are larger or close ($TPC\cdot C_{60}$) to the van der Waals diameter of C_{60} (10.18 Å), therefore, the HOMO–LUMO

Table 5 Donors and their redox potentials. The position of the maximum of CTB (λ/nm) and the $h\nu_{CT}$ energies in the C_{60} complexes in the solid state (the letters correspond to Fig. 15, the numbers correspond to Fig. 16)

Donor	E_{redox}[a]/V	Complex	N	λ/nm	$h\nu_{CT}$/eV
TPDP	+0.15[95]	$D(C_{60})_2(CS_2)_4$	a	1240	0.98
OMTTF	+0.27[96]	$D{\cdot}C_{60}{\cdot}C_6H_6$	2	1040	1.20
		$D{\cdot}C_{60}{\cdot}C_5H_5N$	3	980	1.26
TMPD	+0.12[94]	$D{\cdot}C_{60}$	b	975	1.27
DMDP-TTF	+0.34[96]	$D_2{\cdot}C_{60}{\cdot}C_6H_6$	10	940	1.32
EDY-BEDT-DT	+0.41[96]	$D{\cdot}C_{60}{\cdot}C_6H_6$	11	935	1.32
EDT-TTF	+0.44[23]	$D_2C_{60}{\cdot}CS_2$	12	900	1.35
		$D{\cdot}C_{60}{\cdot}C_6H_6$	13	920	1.38
BEDO-TTF	+0.43[96]	$D{\cdot}C_{60}{\cdot}C_6H_6$	5	900	1.38
DP-TTF	+0.43[97]	$D{\cdot}C_{60}{\cdot}C_6H_6$	14	895	1.38
TMDTDM-TTF	+0.39[96]	$D_2C_{60}(CS_2)_3$	15	900	1.39
BEDT-TTF	+0.53[96]	$D_2C_{60}(C_5H_5N)_2$	6	820	1.51
		D_2C_{60}	7	790	1.57
DBTTF	+0.62[96]	$D{\cdot}C_{60}{\cdot}C_6H_6$	8	735	1.69
		$D{\cdot}C_{60}{\cdot}C_5H_5N$	9	750	1.64
OOT-TTF	+0.66[96]	$D{\cdot}C_{60}{\cdot}C_7H_8$	16	725	1.71
BTX	—	$D{\cdot}C_{60}{\cdot}CS_2$	—	625	1.98
		$D{\cdot}C_{60}$		620	2.00

[a] E_{redox} are determined *vs.* Ag/AgCl in acetonitrile.

overlapping of the adjacent C_{60} molecules is absent or insignificant in these complexes.

Thus the absorption of C_{60} at 420–530 nm seems to be associated with intermolecular electron transitions whose intensity is defined by the HOMO–LUMO overlapping of the adjacent C_{60} molecules. If the distances between the C_{60} molecules are large in the complexes, intermolecular electron transitions become impossible. The same situation is realised for solutions in which the isolation of the C_{60} molecules by solvents results in the disappearance of AB of C_{60} at 450 nm.[88] However, aggregation of several C_{60} molecules in solution (in the complexes with γ-cyclodextrins[90] or calixarenes[91]) results in the appearance of this AB.

3.5.2 Charge transfer bands. Now the processes of charge transfer (CT) in fullerene compounds are intensively studied.[15,92–94] The synthesis of a great number of C_{60} complexes allows the derivation of general dependencies for the CT energies in these compounds. Electronic absorption spectra of the C_{60} complexes were studied both in solution and in the solid state.[83,84]

CTBs in electronic absorption spectra are determined by subtraction of a normalised C_{60} spectrum from that of the complex (Fig. 14). CTBs are wide, asymmetric, and their position depends on the ionisation potentials (E_i) of the donors.

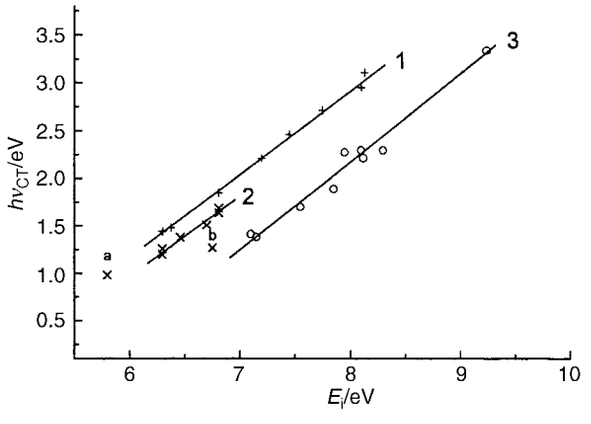

Fig. 15 Dependence of the energy of charge transfer ($h\nu_{CT}$) on E_i of donors for the C_{60} complexes in toluene[84,92,93] (line 1) and for the C_{60} complexes with substituted tetrathiafulvalenes (line 2) and with other donors (a, b, Table 5) in the solid state.[84] A similar dependency for the TCNE complexes with aromatic hydrocarbons in dichloromethane[112] is presented for comparison (line 3).

CT energies corresponding to the maxima of CTB ($h\nu_{CT}$) of the C_{60} complexes are presented in Table 5. Other compounds obtained exhibit CTB of a too weak intensity (less then noise level in this spectral range) and can be attributed to molecular complexes.

For C_{60} complexes with tetrathiafulvalenes, namely, OMTTF, BEDT-TTF, BEDO-TTF, and DBTTF in the solid state, the dependence of the $h\nu_{CT}$ energies on donor E_i is linear (Fig. 15, line 2) and follows the expression: $h\nu_{CT} = 0.82E_i - 3.93$ eV.[84] However, for the C_{60} complexes with donors of other families, namely, TPDP and TMPD, the $h\nu_{CT}$ energies *versus* E_i values (Fig. 15, points a and b) do not fall into this dependency. The similar dependence for the C_{60} complexes in toluene lies 0.2 eV higher than in the solid state[84] (Fig. 15, lines 1 and 2).

The dependence of the $h\nu_{CT}$ energies on the difference in redox potentials of tetrathiafulvalenes and the first reduction potential of C_{60} (Fig. 16) in the C_{60} complexes is also close to linear.

The dependences derived allow the estimation of the positions of CTBs from the known E_i and E_{redox} or the calculations of unknown E_i from the $h\nu_{CT}$ energies.

It seems that the $h\nu_{CT}$–E_i dependence for C_{60} complexes in solutions is similar for various types of organic donors.[84] The analogous dependence in the solid state is valid only for the donors of one family, for example, substituted tetrathiafulvalenes. This is associated with the fact that the donors of one family have close averaged distances between the donor and the

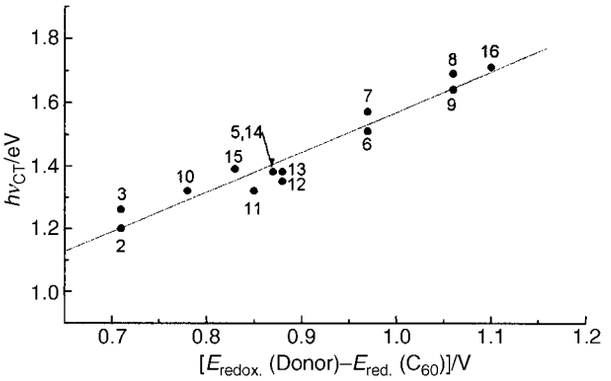

Fig. 16 Dependence of the energy of charge transfer ($h\nu_{CT}$) on the difference of redox potentials of tetrathiafulvalenes and the first reduction potential of C_{60} (−0.44 V).[106] Numbers are given in accordance with Table 5.

Table 6 X-Ray photoelectron spectra: halfwidths of the peaks (ΔC1s and ΔS2p), binding energy of donor heteroatoms and its shift in the complexes with respect to the initial donor. The energy of the σ+π plasmon in the electron energy loss spectrum ($h\omega(\sigma+\pi)$)

N	Complex	ΔC1s/eV	ΔS2p/eV	S2p/eV	Shift S2p/eV	$h\omega_p(\sigma+\pi)$/eV
1	C_{60}	1.8	—	—	—	26.1
2	(EDT-TTF)$_2C_{60}\cdot CS_2$	2.2	2.5	163.9	+0.1	24.6
3	EDT-TTF$\cdot C_{60}\cdot C_6H_6$	2.1	2.5	163.9	+0.1	24.9
4	DP-TTF$\cdot C_{60}\cdot C_6H_6$	1.9	2.7	164.1	0	—
5	(DMDP-TTF)$_2\cdot C_{60}\cdot C_6H_6$	1.9	2.6	164.0	+0.1	—
6	EDY-BEDT-DT$\cdot C_{60}\cdot C_6H_6$	2.0	2.5	164.0	+0.4	24.0
7	BNDY$\cdot C_{60}$	2.0	2.6	164.9 (169.8)	+0.4 (S^{+6})	24.8
8	(TMDTDM-TTF)$_2C_{60}(CS_2)_3$	1.9	2.5	163.8	+0.1	24.0
9	DBTTF$\cdot C_{60}\cdot C_6H_6$	1.95	2.4	164.3	+0.3	25.3
10	(BEDO-TTF)$_2C_{60}$	2.3	2.6	164.0	+0.7	24.0
11	TMT$(C_{60})_3C_6H_6$	2.0	2.7	164.0	+1.0	25.2
12	(TMT)$_2C_{60}(C_7H_8)_{0.5}$	2.4	2.7	163.9	+0.9	23.9
13	(BA)$_2C_{60}$	2.3	—	—	—	24.8
14	$S_4N_4\cdot C_{60}$	—	—	165.4 (169.5)	+0.6 (S^{+6})	—
15	$(S_4N_4)_{0.9}C_{60}(C_6H_6)_{1.1}$	—	—	165.1 (169.5)	+0.3 (S^{+6})	—
				N1s/eV		
14	$S_4N_4\cdot C_{60}$	—	—	399.2	+1.2	—
15	$(S_4N_4)_{0.9}C_{60}(C_6H_6)_{1.1}$	—	—	399.6	+1.6	—
				$Te3d_{5/2}$/eV		
16	BTX $\cdot C_{60}\cdot CS_2$	—	—	574.1	+0.2	25.2

Parameters and attribution of the additional peaks in the XP-spectra are given in brackets.

C_{60} molecules in the crystal and consequently close energies of electrostatic interaction in excited state.

3.6 X-Ray photoelectron spectroscopy

X-Ray photoelectron spectroscopy (XPS) is a sensitive method for the determination of the atomic composition of compounds and the valence state of elements in thin surface layers. Based on the shifts of the line position of heteroatoms of the donors contained in the complex and in the individual state it is possible to estimate the redistribution of electron density upon formation of the D–A complex.

The data of XP-spectra[98–100] for the C_{60} complexes are presented in Table 6.

The position of the S2p peak coincides within the experimental error (±0.1 eV) for most complexes and the starting donors, indicating the absence of charge transfer.[98,99] Noticeable positive shifts of the peaks S2p (0.3–0.9 eV), N1s (0.8–1.6 eV), and $Te3d_{5/2}$ (0.4 eV) are also observed for some complexes, which could be evidence for electron density transfer from the donor to fullerene. However, the calibration of the XP-spectra as to the peak C1s (285.0 eV) is not perfect. The intensity of the peak C1s in the complexes is defined mainly by fullerene molecules, while in the spectra of starting donors the main contribution can be made by charged carbon atoms. In this case, the position of the peak of a donor heteroatom is shifted.[98,99]

The energy of σ+π plasmons ($h\omega_p$) corresponding to excitation of plasma oscillations of all valence electrons is lower in the complexes than in the starting C_{60} (26.1 eV). Providing $h\omega_p=(4\pi ne^2m^{-1})^{1/2}$ (n is valence electron density, m and e are electron mass and charge, respectively), the valence electron density must also be lower in the complexes than in the starting C_{60}. This assumption is confirmed by the calculations of valence electron density for complexes with known structures.[59]

Fig. 17 shows the C1s spectra of TPC(1), TPC$\cdot C_{60}$ (2), and C_{60} (3). A satellite structure is observed in all the spectra at higher energies relative to the basic C1s peak. In TPC the distance between the basic and the satellite peaks is 6.7 eV. The satellite peak is attributed to the excitation of the π–π* electron transitions in the TPC phenylene groups. For the satellite structures of C_{60} and TPC$\cdot C_{60}$, the distance between these peaks is smaller and equal to 3.1 eV. Therefore, the nature of the satellite peaks is different in the starting TPC and TPC$\cdot C_{60}$. The π–π* electronic transitions of the TPC phenylene groups are not manifested in the satellite structure of the C1s spectrum of the complex.[55] This can be associated with a strong interaction of the π-electrons of C_{60} and the TPC phenylene groups. Similar effects were observed in the C_{60} complexes with DAN[54] and BA.

The XP-spectra demonstrated that the surface of the crystals of some C_{60} complexes involves donor heteroatoms in both basic and higher oxidation states.[100] For example, the S2p

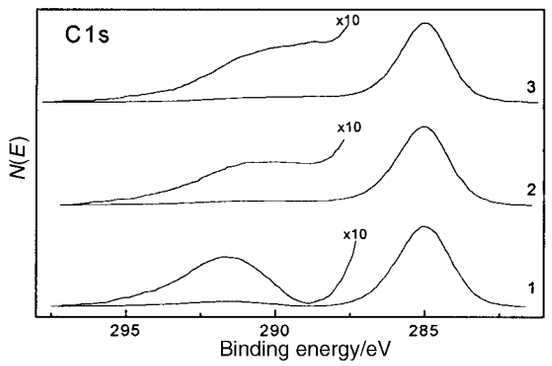

Fig. 17 The peaks C1s in XP-spectra of TPC (1), TPC$\cdot C_{60}$ (2), and C_{60} (3) (Reprinted from Ref. 55, Copyright 1998, Elsevier).

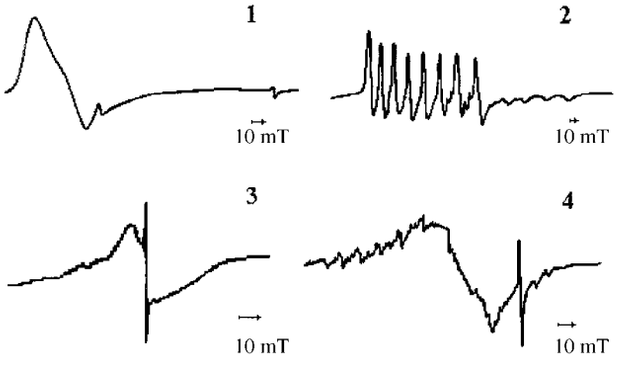

Fig. 18 EPR spectra of MnTPP (1), CoTPP (2), MnTPP$(C_{60})_2(CS_2)_{1.5}$ (3), and CoTPP$C_{60}(CS_2)_{0.5}$ (4). The signals with $g=2.0022$ and $\Delta H=2$ G in the spectra of the complexes are attributed to the "defect" signal of C_{60}.

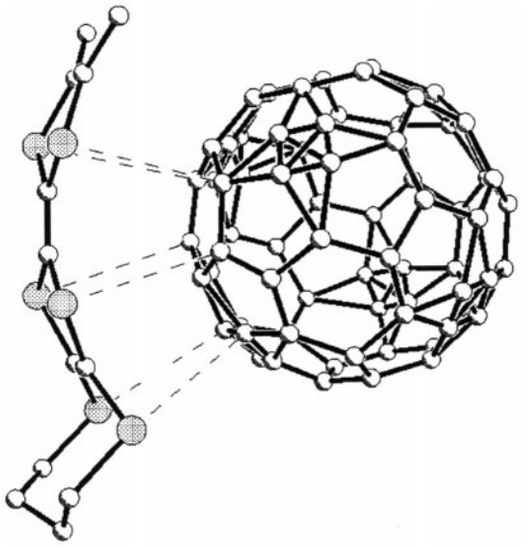

Fig. 19 Coordination of TMDTDM-TTF molecule to C_{60} one in $(TMDTDM\text{-}TTF)_2C_{60}(CS_2)_3$ (Reprinted from Ref. 57, Copyright 1997, Elsevier).

spectra of the $BNDY{\cdot}C_{60}$, $(S_4N_4)_{0.9}C_{60}(C_6H_6)_{1.1}$, and BEDO-$TTF{\cdot}C_{60}{\cdot}C_6H_6$ crystals show a peak with binding energy $E_b = 169.8$ eV in addition to the basic peak with $E_b = 164.1$ eV. The position of the additional peak corresponds to the state S^{6+}. Solid S_4N_4, BNDY, and BEDO-TTF are stable enough to oxygen for either long-duration storage or recrystallisation under conditions of the complex preparation. The appearance of highly oxidised donor heteroatoms on the surface of the crystals of complexes seems to be due to the presence of fullerene, which could perform as a catalyst of oxidation and/or carrier of active oxygen.[100]

3.7 EPR Spectra

The EPR spectra of fullerene complexes show the presence of the weak EPR signal with $g = 2.0022$ and $\Delta\boldsymbol{H} = 1.5$–2 G at room temperature, which remains almost unchanged down to liquid helium temperatures. This EPR signal appears even in the samples of starting C_{60} and is associated with defects resulting from fullerene oxidation by atmospheric oxygen.[101–103] The signal is not intense (10^{-4}% of the sample mass). However, on heating the C_{60} sample in air the intensity of the signal increases by orders of magnitude.[102] The intensity of the "defect" EPR signal in the complexes depends on the methods of complex preparation and storage. This "defect" signal was not considered in further discussion.

It is known[104,105] that the C_{60} radical anion yields the signal with $g = 1.996$–1.999 and $\Delta\boldsymbol{H} = 20$–50 G at room temperature, which strongly narrows with the temperature decrease. Since the reduction potential of C_{60} is -0.44 V in dichloromethane *vs.* SCE,[106] formation of complexes with noticeable charge transfer can be expected only for strong enough donors ($E_{redox} < +0.3$ V). Therefore, there is no signal attributed to $C_{60}^{-\cdot}$ in the spectra of most of complexes obtained.

The formation of $(Cp_2Ni)_xC_{60}(CS_2)_2$, where $x < 0.2$, is accompanied by the appearance of two new signals, which are absent in the EPR spectra of the starting compounds. The signal with $g = 2.117$ and $\Delta\boldsymbol{H} = 13.5$ G at 300 K can be attributed to Cp_2Ni^+. The temperature decrease down to 77 K yields the splitting into three signals with $g = 2.109$ and $\Delta\boldsymbol{H} = 20$ G; $g = 2.090$ and $\Delta\boldsymbol{H} = 10$ G; $g = 2.064$ and $\Delta\boldsymbol{H} = 25$ G which can be the three components of an anisotropic signal (x, y, and z, respectively). It is known that the Cp_2Ni^+ cation has an anisotropic EPR signal in the $Cp_2Co^+PF_6^-$ matrix with $g_x = 1.972$, $g_y = 2.015$, and $g_z = 1.800$ (4 K).[107] Larger values of g-factors in $(Cp_2Ni)_xC_{60}(CS_2)_2$ ($x < 0.2$) can be associated with the interaction of Cp_2Ni^+ with the C_{60} molecules. The signal with $g = 2.0000$ and $\Delta\boldsymbol{H} = 30$ G (300 K) can be attributed to the $C_{60}^{-\cdot}$ radical anion. Small intensity of the ESR signals seems to be associated with a small amount of nickelocene in the complex and only partial charge transfer from nickelocene to C_{60}.

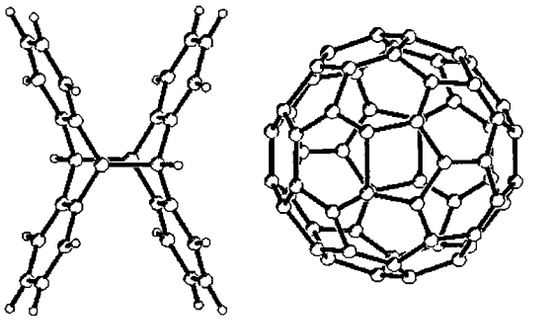

Fig. 20 Coordination of DAN molecule to C_{60} molecule[54] in $DAN{\cdot}C_{60}(C_6H_6)_3$ (Reprinted from Ref. 54, Copyright 1997, Royal Society of Chemistry).

In spite of strong enough donor properties of Mn(II) and Co(II) tetraphenylporphyrins in $Mn(TPP)(C_{60})_2(CS_2)_{1.5}$ and $Co(TPP)C_{60}(CS_2)_{0.5}$, there is no electron transfer to the C_{60} molecule.[62] One observes only the changes in electronic state of the central metal cation. These changes are obviously due to a strong interaction of d-orbitals of metal and π-orbitals of C_{60}. For example, $Mn(TPP)(C_{60})_2(CS_2)_{1.5}$ has a singlet signal with $g = 2.002$ and $\Delta\boldsymbol{H}_{pp} = 250$ G at 77 K characteristic of low-spin state of Mn(II) with $S = 1/2$,[62] which differs strongly from the EPR signal of the starting Mn(TPP) ($g_\perp = 5.9$ and $g_\parallel = 2.0$, $S = 5/2$, 77 K[108]) (Fig. 18.1 and 3). The decrease of spin concentration of $Mn(TPP)(C_{60})_2(CS_2)_{1.5}$ is seen as a hyperfine structure from the ^{14}N nuclei indicating that the spin density of Mn(II) in the complex is delocalized also on the nitrogen atoms of the pyrrole ring of MnTPP. $CoTPP{\cdot}C_{60}(CS_2)_{0.5}$ manifests an asymmetric EPR signal (Fig. 18.4) with $\langle g \rangle = 2.4$ and $\Delta\boldsymbol{H}_{pp} = (500-600)$ G from parallel and perpendicular spectral components[62] which also differs from the EPR signal of the starting CoTPP ($g_\perp = 3.322$, $B = 395 \times 10^{-4}$ cm^{-1}, $g_\parallel = 1.798$, $A = 197 \times 10^{-4}$ cm^{-1}) (Fig. 18.2 and 4).[109]

3.8 Peculiarities of donor–C_{60} interactions

Donor–acceptor (D–A) complexes are formed due to relatively weak van der Waals interactions and the forces of charge transfer from donors to acceptors.[110]

The degree of charge transfer in the D–A complexes is mainly defined by the difference of vertical ionisation potentials (E_i) of donors and electron affinity (E_{ea}) of acceptors together with the efficiency of the HOMO–LUMO overlap.[110]

A study of the acceptor ability of fullerenes was carried out using various methods. It is reported[111] that vertical E_{ea} of C_{60} is 2.67 eV in the gas phase.

However, the dependence of charge transfer energy on E_i of donors in the C_{60} complexes in solution lies 0.6–0.7 eV higher[84] than that in the TCNE complexes[112](Fig. 15, line 2 and 3) (E_{ea} of TCNE is 2.77 eV[113]). Thus in spite of high E_{ea} in the gas phase, fullerene C_{60} show rather weak acceptor properties in solution.

Effective HOMO–LUMO overlap in the π-complexes is realised if the π-orbitals of donors and acceptors are parallel to each other and located at a distance less than the sum of the van der Waals radii of the corresponding atoms.[110]

Fig. 19 shows the coordination of TMDTDM-TTF to a C_{60} molecule in $(TMDTDM\text{-}TTF)_2C_{60}(CS_2)_3$. The starting TMDTDM-TTF molecule is planar (excluding methylene groups), while in the complex it has a boat conformation with dihedral angles of 27.1 and 23.8° between the central S_4C_2

fragment and the outer planes. Such a change in the conformation partially breaks the π-conjugation in the molecule and decreases its donor properties.

At the coordination of TMDTDM-TTF to C_{60}, the S_4C_2 fragment forms a dihedral angle of 12° with hexagonal faces of C_{60} and S···C (C_{60}) distances 3.412–3.793 Å. The values of dihedral angles are 20–30° for the outer planes of TMDTDM-TTF and the faces of C_{60}. Therefore, the efficiency of the π–π overlap of TMDTDM-TTF and C_{60} molecules is low in the complex. Because of the large dihedral angles between the planes of the molecules, only three S atoms of the donors have shortened van der Waals contacts with the C_{60} carbons (less than 3.55 Å).[57] Similar coordination of DBTTF to C_{60} was observed in DBTFF·C_{60}·C_6H_6.[59]

In TPDP the phenyl groups are rotated by angles of 10.2 and 7.6° relative to the plane of the dipyranylidene fragment.[68] Its coordination to the C_{60} molecule in TPDP$(C_{60})_2(CS_2)_4$ results in strong distortion of TPDP (an angular deviation of the phenyl rings from the plane of the dipyranylidene fragment is 33°) and a partial breakdown of π-conjugation in the molecule.[67]

The dihedral angles between the phenyl groups of TPDP and the C_{60} faces are 19 and 25°, therefore only two or three carbon atoms of phenyl groups have shortened (C)···(C) distances with C_{60}. As a result, charge transfer from TPDP to C_{60} can be also hindered.

Noncomplementarity of the shapes of initially planar donors and the spherical C_{60} molecule is the main cause for the distortion of donor molecules and low efficiency of π-orbitals overlapping.

Thus, charge transfer is insignificant in the complexes obtained and they are formed mainly due to van der Waals polarisation forces because of the high polarisability of fullerenes ($\alpha \sim 85$ Å^3)[114] and donors, for example, tetrathiafulvalenes[115] have $\alpha \sim 20$–40 Å^3. The polarisation interaction causes the distortion of planar tetrathiafulvalene and dipyranylidene molecules in the complexes. The energy required for the distortion and partial breakdown of π-conjugation must be balanced by a more efficient polarisation interaction of π-electron clouds of donors and C_{60} at their closer approach.

"Concave" donor molecules such as DAN, BTX, and BA are able to approach the C_{60} molecule without changes of the conformation and form with C_{60} multiple van der Waals contacts (Fig. 20). Such complexes are easily crystallised from the dilute solutions.

For example, the reaction of complex formation of C_{60} with dianthracene is realised even in dilute (0.05 mg mL^{-1} of C_{60}) benzene solutions with precipitation of DAN·$C_{60}(C_6H_6)_3$ with a quantitative yield. This reaction can be used for the isolation and quantitative determination of the content of C_{60} in solutions by the weight of the precipitated complex. Pure C_{60} may be isolated from the complex on dissolving DAN·$C_{60}(C_6H_6)_3$ in hot toluene followed by precipitation with acetonitrile or by heating DAN·$C_{60}(C_6H_6)_3$ at 330 °C in argon.

3.9 Conducting properties

Because of the absence of charge transfer, all the complexes are dielectrics whose conductivity is less than 10^{-5} S cm^{-1}. The highest values of conductivity are seen in C_{60} complexes with tetrathiafulvalenes: 10^{-5} to 10^{-6} S cm^{-1}.

4 Conclusion

Complexes of C_{60} with donor molecules of various families, namely, substituted tetrathiafulvalenes, bis(telluraxanthenyl), tetraphenyldipyranylidene, diazodithiafulvalene, tetramethoxythianthrene, aromatic hydrocarbons, tetrasulfur tetranitride, metallocenes, metal(II) tetraphenylporphyrins, and a number of other donors have been obtained. Depending on the size and conformation of the donor component, fullerene molecules are packed in the crystal in one-dimensional chains, two-dimensional layers or they have a three-dimensional arrangement with different distances between them.

The estimation of the degree of charge transfer (δ) in the complexes from the shifts of its AB at 1429 cm^{-1} in the IR spectra showed them to have a neutral ground state. The IR spectra of some complexes manifested the symmetry-forbidden vibrations of C_{60}. The splitting of the absorption bands of C_{60} is attributed to the freezing of the rotation of C_{60} molecules on interaction with donor molecules.

The electronic spectra of the C_{60} complexes with tetrathiafulvalenes, amines, and dipyranylidenes show bands at 620–1240 nm attributed to electron transfer from the donor to C_{60} with the absorption of a light quantum. The presence of charge transfer bands allows these compounds to be considered as charge transfer complexes. The energies of charge transfer ($h\nu_{CT}$) in the C_{60} complexes with tetrathiafulvalenes in the solid state have been shown to depend linearly on the ionisation potentials of the donors and lie lower by 0.2 eV than in solution. The $h\nu_{CT}$–E_i dependence for the C_{60} complexes in solution lies higher by 0.6–0.7 eV than that for TCNE ones.

The increased distances between the C_{60} molecules in the complexes result in a decrease in intensity of the C_{60} absorption at 420–530 nm, which allows us to attribute this absorption to intermolecular HOMO–LUMO transitions between the adjacent C_{60} molecules.

According to the XP-spectra the transfer of electron density in most of the complexes is either absent or insignificant. However noticeable positive shifts of the peaks of donor heteroatoms in the complexes (up to 1.6 eV) were also observed.

The redox potentials of the donors used by us are not high enough to reduce C_{60} to $C_{60}^{-\cdot}$ radical anion (E_{red} of C_{60} is −0.44 V[106]). However, we could expect the formation of molecular complexes and complexes with a different degree of charge transfer.

However, the degree of charge transfer in the complexes is almost independent of ionization or redox potentials of donors. Even for such strong donors as MnTPP ($E_{redox} = -0.23$ V),[116] Cp*$_2$Fe ($E_{redox} = -0.09$ V),[117] DADTF ($E_{redox} = -0.05$ V),[118] and TPDP ($E_{redox} = +0.15$ V)[95] the degree of charge transfer is close to zero.

Only $(Cp_2Ni)_xC_{60}(CS_2)_2$ ($x < 0.2$) have weak ESR signals from the $C_{60}^{-\cdot}$ radical anions in the ground state. The formation of the complexes with metal(II) tetraphenylporphyrins results only in significant changes in electronic state of a metal atom probably due to the interaction with C_{60}.

The basic factor of the effective charge transfer and van der Waals interaction in the C_{60} complexes is a steric complementarity of the shapes of donor molecules to the spherical surface of C_{60} ones. This criterion is valid for small donor molecules, which are not sensitive to the spherical surface of fullerene and can coordinate to one of the faces of C_{60} (Cp_2Ni, S_4N_4 and TMPD).

Concave donor molecules, for example, "double butterfly"-shaped BA, BTX, BXA, and DAN molecules; TPC molecule (involving three phenylene groups at an angle of 120°), and TMT molecule (involving two planar fragments arranged at an angle of 128°)[119] are not strong donors, however, are capable of forming complexes with C_{60} with strong van der Waals interaction.

To coordinate to C_{60} planar donors must be flexible (substituted tetrathiafulvalenes, namely, TMDTDM-TTF, BEDO-TTF, EDT-TTF, BEDT-TTF, and donors EDT-BEDT-DT and BNDY) or include labile phenyl groups (TPDP, DTDAF, TBMA, MeTPP, TPE, and TPB) (Fig. 1). However, in this case a strong distortion of donor conformation and hindrance to charge transfer are observed.

The absence of charge transfer in the complexes defines their dielectric properties. Further studies of C_{60} complexes can be concerned with the changes in their neutral state. The neutral state of the complexes can be changed either by photoinduced electron transfer or intercalation by oxidants and reductants. Photoinduced electron transfer in neutral complexes results in an excited ionic state. Intercalation processes[13,14,120,121] yield ionic three-component systems, $D^+\cdot(C_{60})An^-$ or $D\cdot(C_{60}{}^{n-})nK^+$, where An^- and K^+ are anion and cation, respectively. An important problem is the preparation of such three-component systems *in situ* in solutions.[122] The ionic state results in essential changes in the physical properties of the complexes and the fabrication of materials with unusual magnetic and conducting (superconducting) properties.

Acknowledgements

The work was supported by the Russian Program "Fullerenes and Atomic Clusters".

References

1 H. W. Kroto, J. R. Heath, S. C. O'Brien, R. F. Curl and R. E. Smalley, *Nature*, 1985, **318**, 162.
2 M. S. Dresselhaus, G. Dresselhaus and P. C. Eklund, *Science of Fullerenes and Carbon Nanotubes*, Academic Press, San Diego, 1996.
3 D. V. Konarev and R. N. Lyubovskaya, *Russ. Chem. Rev.*, 1999, **68**, 19.
4 (*a*) A. L. Balch and M. M. Olmstead, *Chem. Rev.*, 1998, **98**, 2123; (*b*) N. Martin, L. Sánchez, B. Illescas and I. Pérez, *Chem. Rev.*, 1998, **98**, 2527; (*c*) E. Echegoyen and L. E. Echegoyen, *Acc. Chem. Res.*, 1998, **31**, 593.
5 M. J. Rosseinsky, *J. Mater. Chem.*, 1995, **5**, 1497.
6 M. J. Rosseinsky, *Chem. Mater.*, 1998, **10**, 2665.
7 K. Tanigaki and K. Prassides, *J. Mater. Chem.*, 1995, **5**, 1515.
8 V. Buntar, F. M. Sauerzopf and H. W. Weber, *Aust. J. Phys.*, 1997, **50**, 359.
9 H. Moriyama, H. Kobayashi, A. Kobayashi and T. Watanabe, *Chem. Phys. Lett.*, 1995, **238**, 116.
10 M. Ricco, M. Bisbiglia, R. Derenzi and F. Bolzoni, *Solid State Commun.*, 1997, **101**, 413.
11 P. W. Stephens, D. Cox, J. W. Lauher, L. Mihaly, J. B. Wiley, P.-M. Allemand, A. Hirsch, K. Holczer, Q. Li, J. D. Thompson and F. Wudl, *Nature (London)*, 1992, **355**, 331.
12 H. Wang and D. Zhu, *Solid State Commun.*, 1995, **93**, 295.
13 A. Otsuka, G. Saito, T. Teramoto, Y. Sunari, T. Ban, A. A. Zakhidov and K. Yakushi, *Mol. Cryst. Liq. Cryst.*, 1996, **284**, 345.
14 A. Otsuka, G. Saito, S. Hirate, S. Pac, T. Ishida, A. A. Zakhidov and K. Yakushi, *Mater. Res. Soc. Symp. Proc.*, 1998, **488**, 495.
15 N. S. Sariciftci and A. J. Heeger, in *Handbook of organic conductive molecules and polymers*, ed. H. S. Nalwa, John Wiley and Sons Ltd., 1997, vol. 1, p. 414.
16 V. A. Nadtochenko, A. A. Moravsky, V. V. Gritsenko, G. V. Shilov and O. A. Dyachenko, in *Abstracts of International Workshop "Fullerenes and Atomic Clusters" (IWFAC-95)*, St. Petersburg, 1995, 53.
17 V. V. Kveder, E. A. Steinman, B. Zh. Narimbetov, S. S. Khasanov, L. P. Rozenberg, R. P. Shibaeva, A. V. Bazhenov, A. V. Gorbunov, M. Yu. Maksimuk, D. V. Konarev, R. N. Lyubovskaya and Yu. A. Ossipyan, *Chem. Phys.*, 1997, **216**, 407.
18 F. Kajzar, Y. Okada-Shudo, C. Meritt and Z. Kafafi, *Synth. Met.*, 1998, **94**, 91.
19 R. E. Douthwaite, M. L. H. Green, S. J. Heyes, M. J. Rosseinsky and J. F. C. Turner, *J. Chem. Soc., Chem. Commun.*, 1994, 1367.
20 G. Roth and P. Adelmann, *Appl. Phys., A: Solids Surf.*, 1993, **56**, 169.
21 P. R. Birkett, C. Christides, P. B. Hitchcock, H. W. Kroto, K. Prassides, R. Taylor and D. R. M. Walton, *J. Chem. Soc., Perkin Trans. 2*, 1993, 1407.
22 A. Izuoka, T. Tachikawa, T. Sugawara, Y. Suzuki, M. Konno, Y. Saito and H. Shinohara, *J. Chem. Soc., Chem. Commun.*, 1992, 1472.
23 G. Saito, T. Teramoto, A. Otsuka, Y. Sugita, T. Ban, M. Kusunoki and K.-I. Sakaguchi, *Synth. Met.*, 1994, **64**, 359.
24 O. A. D'yachenko and S. V. Konovalikhin, *Koord. Khim.*, 1998, **24**, 700.
25 S. V. Konavalikhin, O. A. D'yachenko, G. V. Shilov, N. G. Spitsina, K. V. Van and E. B. Yagubskii, *Izv. AN, Ser. Khim.*, 1997, 1480.
26 J. Llacay, J. Tarres, C. Rovira, J. Veciana, M. Mas and E. Molins, *J. Phys. Chem. Solids*, 1997, **58**, 1675.
27 P. Wang, W.-J. Lee, I. Scherbakova, M. P. Cava and R. M. Metzger, *Synth. Met.*, 1994, **64**, 319.
28 Y. Li, Y. Gao, F. Bai, Y. Mo, B. Zhang, H. Han and D. Zhu, *Synth. Met.*, 1995, **70**, 1459.
29 A. Izuoka, T. Tachikawa, T. Sugawara, Y. Saito and H. Shinohara, *Chem. Lett.*, 1992, 1049.
30 J. L. Atwood, M. J. Barnes, M. G. Gardiner and C. L. Raston, *J. Chem. Soc., Chem. Commun.*, 1996, 1449.
31 J. W. Steed, P. C. Junk, J. L. Atwood, M. J. Barnes, C. L. Raston and R. S. Burkhalter, *J. Am. Chem. Soc.*, 1994, **116**, 10346.
32 L. Y. Chiang, J. W. Swirczewski, K. Liang and J. Miller, *Chem. Lett.*, 1994, 981.
33 K. Tsubaki, K. Tanaka, T. Kinoshita and K. Fuji, *Chem. Commun.*, 1998, 895.
34 L. J. Barbour, G. W. Orr and J. L. Atwood, *Chem. Commun.*, 1997, 1439.
35 T. Haino, M. Yanase and Y. Fukazawa, *Angew. Chem., Int. Ed. Engl.*, 1997, **36**, 259.
36 K. N. Rose, L. J. Barbour, G. W. Orr and J. L. Atwood, *Chem. Commun.*, 1998, 407.
37 V. A. Nadtochenko, V. V. Gritsenko, O. A. D'yachenko, G. V. Shilov and A. P. Moravskii, *Izv. AN, Ser. Khim.*, 1996, 1285.
38 A. V. Bazhenov, M. Yu. Maksimuk, T. N. Fursova, A. P. Moravskii and V. A. Nadtochenko, *Izv. AN, Ser. Khim.*, 1996, 1459.
39 L. Golič, R. Blinc, P. Cevc, D. Arčon, D. Mifailovič, A. Omerzu and P. Venturini, in *Fullerenes and Fullerene Nanostructures*, eds. H. Kuzmany, J. Fink, M. Mehring and S. Roth, World Scientific, Singapore, 1997, p. 531.
40 D. M. Eichhorn, S. Yang, W. Jarrell, T. F. Baumann, L. S. Beall, A. J. P. White, D. J. Williams, A. G. M. Barrett and B. M. Hoffman, *J. Chem. Soc., Chem. Commun.*, 1995, 1703.
41 A. I. Kotov, S. V. Konovalikhin, R. I. Pisarev, G. V. Shilov, O. A. D'yachenko and E. B. Yagubskii, *Mendeleev Commun.*, 1994, 180.
42 O. Ermer, *Helv. Chim. Acta*, 1991, **74**, 1339.
43 I. E. Grey, M. J. Hardie, T. J. Ness and C. L. Raston, *Chem. Commun.*, 1999, 1139.
44 M. Fedurco, M. M. Olmstead and W. R. Fawcett, *Inorg. Chem.*, 1995, **34**, 390.
45 J. D. Crane, P. B. Hitchcock, H. W. Kroto, R. Taylor and D. R. M. Walton, *J. Chem. Soc., Chem. Commun.*, 1992, 1764.
46 W. C. Wan, X. Liu, G. M. Sweeney and W. E. Broderick, *J. Am. Chem. Soc.*, 1995, **117**, 9580.
47 A. L. Balch, J. W. Lee, B. C. Noll and M. M. Olmstead, in *Recent Advances in the Chemistry and Physics of Fullerenes and Related Materials*, ed. K. M. Kadish and R. S. Ruoff, *Electrochemical Society Proceedings*, Pennington, NJ, 1994, vol. 94-24, p. 1231.
48 J. D. Crane and P. B. Hitchcock, *J. Chem. Soc., Dalton Trans*, 1993, 2537.
49 A. Penicaud, J. Hsu, C. A. Reed, A. Koch, K. Khemani, P. M. Allemand and F. Wudl, *J. Am. Chem. Soc.*, 1991, **113**, 6698.
50 M. J. Hardie and C. L. Raston, *Chem. Commun.*, 1999, 1153.
51 P. N. Saeta, B. I. Greene, A. R. Kortan, N. Kopylov and F. A. Thiel, *Chem. Phys. Lett.*, 1992, **190**, 184.
52 D. V. Konarev, R. N. Lyubovskaya, O. S. Roschupkina, Yu. M. Shul'ga, M. G. Kaplunov, I. N. Kremenskaya, L. P. Rozenberg, S. S. Khasanov and R. P. Shibaeva, *Mendeleev Commun.*, 1996, 3.
53 D. V. Konarev, R. N. Lyubovskaya, O. S. Roschupkina, Yu. M. Shul'ga, M. G. Kaplunov, I. N. Kremenskaya, L. P. Rozenberg, S. S. Khasanov and R. P. Shibaeva, *Mol. Mater.*, 1996, **8**, 79.
54 D. V. Konarev, E. F. Valeev, Yu. L. Slovokhotov, Yu. M. Shul'ga and R. N. Lyubovskaya, *J. Chem. Res. (S)*, 1997, 442.
55 D. V. Konarev, Yu. V. Zubavichus, E. F. Valeev, Yu. L. Slovokhotov, Yu. M. Shul'ga and R. N. Lyubovskaya, *Synth. Met.*, 1999, **103**, 2364.
56 D. V. Konarev, R. N. Lyubovskaya, O. S. Roschupkina and Yu. M. Shul'ga, *Russ. Chem. Bull.*, 1997, **46**, 32.
57 D. V. Konarev, E. F. Valeev, Yu. L. Slovokhotov,

Yu. M. Shul'ga, O. S. Roschupkina and R. N. Lyubovskaya, *Synth. Met.*, 1997, **88**, 285.
58 D. V. Konarev, Yu. M. Shul'ga, O. S. Roschupkina and R. N. Lyubovskaya, *J. Phys. Chem. Solids*, 1997, **58**, 1869.
59 D. V. Konarev, Y. V. Zubavichus, Yu. L. Slovokhotov, Yu. M. Shul'ga, V. N. Semkin, N. V. Drichko and R. N. Lyubovskaya, *Synth. Met.*, 1998, **92**, 1.
60 D. V. Konarev, R. N. Lyubovskaya, O. S. Roschupkina and Yu. M. Shul'ga, *Russ. Chem. Bull.*, 1995, **44**, 1985.
61 D. V. Konarev, O. S. Roschupkina, M. G. Kaplunov, Yu. M. Shul'ga, E. I. Yudanova and R. N. Lyubovskaya, *Mol. Mater.*, 1996, **8**, 83.
62 E. I. Yudanova, D. V. Konarev, R. N. Lyubovskaya and L. L. Gumanov, *Russ. Chem. Bull.*, 1999, 718.
63 G. A. Domrachev, B. S. Kaverin and V. L. Karnatsevich, in *Abstracts of International Workshop "Fullerenes and Atomic Clusters" (IWFAC-97)*, St. Petersburg, 1997, 252.
64 M. V. Korobov, A. L. Mirakyan, N. V. Avramenko, G. Olofsson, A. L. Smith and R. S. Ruoff, *J. Phys. Chem. B*, 1999, **103**, 1339.
65 A. L. Balch, J. W. Lee, B. C. Noll and M. M. Olmstead, *J. Chem. Soc., Chem. Commun.*, 1993, 345.
66 K. Sh. Karaev, N. G. Furmanov, N. V. Belov, I. D. Sadekov, A. A. Ladatko and V. I. Minkin, *Zh. Strukt. Khim.*, 1981, **22**, 1670.
67 B. Zh. Narimbetov, S. S. Khasanov, L. V. Zorina, L. P. Rozenberg, R. P. Shibaeva, D. V. Konarev and R. N. Lyubovskaya, *Crystallogr. Rep.*, 1997, **42**, 783.
68 P. D. Casseau, J. Gaultier and C. Hauw, *Acta Crystallogr., Sect. B*, 1982, **38**, 1629.
69 D. V. Konarev, E. F. Valeev, Yu. L. Slovokhotov and R. N. Lyubovskaya, *J. Phys. Chem. Solids*, 1997, **58**, 1865.
70 M. L. De Lucia and P. Coppens, *Inorg. Chem.*, 1978, **17**, 2336.
71 I. S. Neretin, Yu. L. Slovokhotov, A. L. Litvinov, D. V. Konarev and R. N. Lyubovskaya, unpublished results.
72 J. Milliken, T. M. Keller, A. P. Baronavsky, S. N. McElvany, J. H. Callanhan and H. H. Nelson, *Chem. Mater.*, 1991, **3**, 386.
73 D. V. Konarev, V. N. Semkin, A. Graja and R. N. Lyubovskaya, *Mol. Mater.*, 1998, **11**, 35.
74 D. V. Konarev, N. V. Drichko, V. N. Semkin, Yu. M. Shul'ga, A. Graja and R. N. Lyubovskaya, in *Electronic properties of novel materials—progress in molecular nanostructures*, ed. H. Kuzmany, J. Fink, M. Mehring and S. Roth, American Institute of Physics, Woodbury, New York, 1998, p. 357.
75 V. N. Semkin, N. V. Drichko, Yu. A. Kimzerov, D. V. Konarev, R. N. Lyubovskaya and A. Graja, *Chem. Phys. Lett.*, 1998, **295**, 266.
76 R. Winkler, T. Picher and H. Kuzmany, *Z. Phys. B*, 1994, **96**, 39.
77 T. Picher, R. Winkler and H. Kuzmany, *Phys. Rev. B*, 1994, **49**, 15879.
78 D. V. Konarev, V. N. Semkin, A. Graja and R. N. Lyubovskaya, *J. Mol. Struct.*, 1998, **450**, 11.
79 V. A. Starodub, E. M. Gluzman, I. F. Golovkina and O. M. Tsiguleva, *Khim. Fiz.*, 1982, 147.
80 M. C. Martin, X. Du, J. Kwon and L. Mihaly, *Phys. Rev. B*, 1994, **50**, 174.
81 L. R. Narasimhan, D. N. Stoneback, A. F. Hrbard, R. C.Haddon and C. K. N. Patel, *Phys. Rev. B*, 1992, **46**, 2591.
82 D. V. Konarev, V. N. Semkin, R. N. Lyubovskaya and A. Graja, *Synth. Met.*, 1997, **88**, 225.
83 D. V. Konarev, R. N. Lyubovskaya, N. V. Drichko, V. N. Semkin and A. Graja, *Synth. Met.*, 1999, **103**, 2466.
84 D. V. Konarev, R. N. Lyubovskaya, N. V. Drichko, V. N. Semkin and A. Graja, *Chem. Phys. Lett.*, 1999, **314**, 570.
85 J. Hora, P. Pánek, K. Navrátil, B. Handlirová, J. Humliček, H. Sitter and D. Stifter, *Phys. Rev. B*, 1996, **54**, 5106.
86 A. V. Bazhenov, A. V. Gorbunov, M. Yu. Maksimuk and T. N. Fursova, *Zh. Eksp. Teor. Fiz.*, 1997, **112**, 246.
87 M. Ichida, A. Nakamura, H. Shinohara and Y. Saito, *Chem. Phys. Lett.*, 1998, **289**, 579.
88 H. J. Byrne, in *Physics and chemistry of fullerenes and derivatives*, eds. H. Kuzmany, J. Fink, M. Mehring and S. Roth, World Scientific, Singapore, 1995, p. 183.
89 P. A. Heiney, J. E. Fischer, A. R. McGhie, W. J. Romanov, A. M. Denenstein, J. P. McCauley, Jr., A. B. Smith III and D. E. Cox, *Phys. Rev. Lett.*, 1991, **67**, 1468.
90 M. Sundahl, T. Anderson and O. Wennerstroem, *Recent Advances in the Chemistry and Physics of Fullerenes and Related Materials*, ed. K. M. Kadish and R. S. Ruoff, *Electrochemical Society Proceedings*, Pennington, NJ, 1994, vol. 94-24, p. 880.
91 C. L. Raston, J. L. Atwood, P. J. Nichols and I. B. N. Sudria, *J. Chem. Soc., Chem. Commun.*, 1993, 2615.
92 S. P. Sibley, R. L. Campbell and H. B. Silber, *J. Phys. Chem.*, 1995, **99**, 5274.
93 R. D. Scurlock and P. R. Ogilby, *J. Photochem. Photobiol. A: Chem.*, 1995, **91**, 21.
94 V. A. Nadtochenko, N. N. Denisov and P. P. Levin, *Russ. Chem. Bull.*, 1995, **44**, 1038.
95 S. Hunig, G. Kleslich, H. Quast and O. Scheutzov, *Liebigs Ann. Chem.*, 1973, 1036.
96 V. Khodorovsky, A. Edžifna and O. Neilands, *J. Mol. Electron.*, 1989, **5**, 33.
97 G. Schukat, L. Van Hinh and E. Fanghänel, *Z. Chem.*, 1976, **16**, 360.
98 Yu. M. Shul'ga, R. N. Lyubovskaya and D. V. Konarev, *Zh. Fiz. Khim.*, 1997, **71**, 2188.
99 Yu. M. Shul'ga, R. N. Lyubovskaya and D. V. Konarev, *Phys. Low-Dim. Struct.*, 1997, **1/2**, 103.
100 Yu. M. Shul'ga, R. N. Lyubovskaya and D. V. Konarev, *Synth. Met.*, 1999, **102**, 1490.
101 J. Stankowski, P. Byszewski, W. Kempinski, Z. Trybuka and N. Zuk, *Phys. Status Solidi B*, 1993, **178**, 221.
102 M. D. Pace, T. C. Christidis, J. J. Yin and J. Millikin, *Phys. Chem.*, 1992, **96**, 6858.
103 Y. L. Hwang, C. C. Yang and K. C. Hwang, *J. Phys. Chem.*, 1997, **101**, 7971.
104 P. M. Allemand, G. Spdanov, A. Koch, K. Khemani, F. Wudl, Y. Rubin, F. Diederich, M. M. Alvarez, S. J. Anz and R. L. Whetten, *J. Am. Chem. Soc.*, 1991, **113**, 2780.
105 H. Moriyama and H. Kabayashi, *J. Am. Chem. Soc.*, 1993, **115**, 1185.
106 D. Dubois, K. M. Kadish, S. Flanagan, R. F. Haufler, L. P. F. Chibante and L. J. Wilson, *J. Am. Chem. Soc.*, 1991, **113**, 4364.
107 J. L. Robbins, N. Edelstein, B. Spencer and J. C. Smart, *J. Am. Chem. Soc.*, 1982, **104**, 1882.
108 B. B. Wayland, L. W. Olson and Z. U. Siddiqui, *J. Am. Chem. Soc.*, 1976, **98**, 94.
109 J. M. Assour, *J. Chem. Phys.*, 1965, **43**, 2477.
110 R. S. Mulliken and W. B. Person, in *Molecular Complexes*, Academic Press, New York, 1969.
111 L. S. Wang, J. Conceicao, C. Jim and R. E. Smalley, *Chem. Phys. Lett.*, 1991, **182**, 5.
112 H. Kuroda, M. Kobayashi, M. Kinoshita and S. Takemoto, *J. Chem. Phys.*, 1962, **36**, 457.
113 E. C. M. Chen and W. E. Wentworth, *J. Chem. Phys.*, 1975, **63**, 3183.
114 M. S. Dresselhaus, G. Dresselhaus, A. M. Rao and P. C. Eklund, *Synth. Met.*, 1996, **78**, 313.
115 N. Sato, K. Seki and H. Inokuchi, *J. Chem. Soc., Faraday Trans. 2*, 1981, **77**, 1621.
116 K. Nagai, T. Iyoda, K. Hashimoto and A. Fujishima, in *Abstracts of Nagoya Conference*, Nagoya, Japan, 1996, 118.
117 J. L. Robbins, N. Edelstein, B. Spencer and J. C. Smart, *J. Am. Chem. Soc.*, 1982, **104**, 1882.
118 G. V. Tormos, M. G. Bakker, P. Wang, M. V. Lakshimikantham, M. P. Cava and R. M. Metzger, *J. Am. Chem. Soc.*, 1995, **117**, 8528.
119 H. Bork, A. Rauschenbach, C. Nather, Z. Havlas, A. Gavezzotti and G. Filippini, *Angew. Chem., Int. Ed. Engl.*, 1995, **34**, 76.
120 R. N. Lyubovskaya, D. V. Konarev, E. I. Yudanova, O. S. Roschupkina, Yu. M. Shul'ga, V. N. Semkin and A. Graja, *Synth. Met.*, 1997, **84**, 741.
121 D. V. Konarev, R. N. Lyubovskaya, V. N. Semkin and A. Graja, *Polish J. Chem.*, 1997, **71**, 96.
122 D. V. Konarev, N. V. Drichko, R. N. Lyubovskaya, E. I. Yudanova, Yu. M. Shul'ga, Y. V. Zubavichus and V. N. Semkin, *Russ. Chem. Bull.*, 1999, **48**, 1946.

Paper a907106g